UNIVERSIDAD DE INVESTIGACIÓN DE TECNOLOGÍA EXPERIMENTAL YACHAY

Escuela de Ciencias Químicas e Ingeniería

Micro computed tomography analysis and mineralogical identification of construction samples affected by haloclasty

Trabajo de integración curricular presentado como requisito para la obtención del título de Química.

Autor:

Ana Gabriela Ruiz Castillo

Tutor:

Ph.D. Edward Ebner Ávila Sosa

Co-Tutor:

Ph.D. Yaniel Misael Vázquez Taset

Urcuquí, septiembre 2023

AUTORÍA

Yo, **RUIZ CASTILLO ANA GABRIELA**, con cédula de identidad 1758314585, declaro que las ideas, juicios, valoraciones, interpretaciones, consultas bibliográficas, definiciones y conceptualizaciones expuestas en el presente trabajo; así cómo, los procedimientos y herramientas utilizadas en la investigación, son de absoluta responsabilidad de el/la autora (a) del trabajo de integración curricular. Así mismo, me acojo a los reglamentos internos de la Universidad de Investigación de Tecnología Experimental Yachay.

Urcuquí, septiembre 2023.

Firmado electrónicamente por:
ANA GABRIELA RUIZ CASTILLO

Ana Gabriela Ruiz Castillo

CI: 1758314585

AUTORIZACIÓN DE PUBLICACIÓN

Yo, **RUIZ CASTILLO ANA GABRIELA,** con cédula de identidad 1758314585, cedo a la Universidad de Investigación de Tecnología Experimental Yachay, los derechos de publicación de la presente obra, sin que deba haber un reconocimiento económico por este concepto. Declaro además que el texto del presente trabajo de titulación no podrá ser cedido a ninguna empresa editorial para su publicación u otros fines, sin contar previamente con la autorización escrita de la Universidad.

Asimismo, autorizo a la Universidad que realice la digitalización y publicación de este trabajo de integración curricular en el repositorio virtual, de conformidad a lo dispuesto en el Art. 144 de la Ley Orgánica de Educación Superior

Urcuquí, septiembre 2023.

Firmado electrónicamente por:
ANA GABRIELA RUIZ CASTILLO

Ana Gabriela Ruiz Castillo

CI: 1758314585

Acknowledgments

I want to thank all the people that made this possible. My family, my friends, my professors and classmates. If only one thing had been different, I may not have made it so far.

A special shout out to Rogger Cedeño and Maria Fernanda Vega, who both went through this before I did and made it less scary.

For my thesis, I wish to express my gratitude towards my tutor, Edward Ávila. I would also like to thank Yaniel Vázquez and Daniel Pijal, who both went out to recollect the samples that were analyzed. Likewise, I want to recognize Elizabeth Mariño, for taking the micro-CT images for the reconstruction of the samples. I'm grateful for the laboratory technicians, Sebastián Gallegos, Cristian Panchana and Miguel Larrea, for their help and support. As well as Felipe Carlosama, Jorge Toro and Raisa Torres for their advice and company.

To my laptop, that held out like a champ, thank you for not failing on me... that much.

And finally, thanks to all the chemistry professors I've had along the way, in particular, I would like to mention Carlos Brito, my first chemistry teacher and the best reference for how fun chemistry could be.

Ana Ruiz

Dedication

I want to dedicate this thesis to both of my tutors. I’m glad I got to stumble upon this project and I’m excited to see what more can come out of it. Thank you for all of your patience, recommendations and guidance.

I would also like to dedicate this to my mother. I’m sorry it took so long, but I made it.

Ana Ruiz

Resumen

En esta tesis se analiza la porosidad de 30 muestras de diferentes materiales, clasificados entre: rocas de lava, ladrillos de arcilla, concreto y adoquines. Todas las muestras fueron obtenidas de la ciudad de Ibarra, Ecuador, en particular, de lugares que demostraron variación de coloración en el mismo material. La extracción de los núcleos consideró cubrir un área de la superficie expuesta y la profundidad varió dependiendo del material de origen. Mediante una microtomografía computarizada, se logró reconstruir las muestras digitalmente y procesarlas para obtener información del tamaño, forma, distribución y ubicación de poros en cada muestra. Este método probó ser confiable para la determinación de macro y meso poros, pero no tuvo suficiente resolución para la determinación de microporosidad. Los resultados mostraron que las muestras de concreto y adoquines tuvieron los poros de mayor tamaño. Debido al límite de la resolución, las muestras de arcilla presentaron la menor cantidad de poros, lo cual se presume ser lo contrario de los resultados. Un análisis más de cerca demostró que estas muestras pueden tener poros de hasta menos de 5 µm. Se corroboró que el método de microtomografía computarizada es más confiable para muestras de concreto. Adicionalmente, se logró relacionar la forma de poros con el tamaño y su posición a lo largo de la muestra. En conclusión, se determinó que los poros superficiales fueron formados debido a haloclastia, pero el efecto es agravante debido a las características climáticas de la zona.

Palabras claves: Haloclastia, Concreto, Adoquines, Meteorización por sales, Ladrillo, Lavas, Materiales de construcción

Abstract

In this thesis, the porosity of 30 samples of different materials, classified as: lava rocks, clay bricks, cobblestones and concrete; is studied. All samples were taken from the city of Ibarra, Ecuador, especially from places that exhibited drastic changes in coloration in the same material. The extraction of core samples considered the exposed surface and a certain depth that varied depending on the source. With the use of micro computerized tomography, samples were reconstructed digitally and processed to obtain information on size, shape, distribution and location of pores in each sample. This method proved very reliable for determination of macropores and mesopores but did not have enough resolution for microporosity. Results showed that concrete and cobblestone samples mostly had the largest pores. Due to the resolution limit, clay brick samples seemed to have the least amount of pores, yet under closer analysis, these samples presented pores even smaller than 5 µm. It was confirmed that the method of computed microtomography is more reliable for concrete samples. Additionally, it was possible to relate the shape of pores with their size and position along the sample. In conclusion, it was determined that surface pores were formed due to haloclasty, but the effect is severe due to the climatic characteristics of the zone.

Keywords: Haloclasty, Concrete, Cobblestone, Salt weathering, Brick, Lava Rocks, Construction materials

CONTENTS

List of Figures

List of Tables

1 INTRODUCTION

The selection of materials for construction highly depends on the construction purpose and the required physical and chemical properties of said material given the exposure it might have to exterior forces, in order to avoid mayor deterioration. Every material has an expiration date. Yet, despite deterioration is unavoidable, it can be slowed down significantly. As material science advances, the incorporation of a multidisciplinary approach towards the study of material performance gives an undeniably better understanding of the deterioration methods and the options available for protection against these processes that weaken various constructions. One of the end goals would be to reduce the frequency of required repairs and retouches, while the other would be to save money in the long run.

In Ecuador, the construction sector accounts for one of the largest economical groups the country. Most materials are elaborated and used for constructions all over the country. Since Ecuador is a volcanic region, the rocks from which many materials are elaborated are volcanic rocks. This poses a significant difference with the source of materials used in other countries, which tends to be mostly from sedimentary rocks. Most of Ecuador's regulations are based on guidelines developed in the United States of America. Therefore, it becomes important to study the mineralogical characteristics of the rocks available here and their impact of the elaboration of materials for construction given the needs of the area.

Since a great part of the territory is rural, many constructions do not even uphold to the national norm established by the government, and many houses are self-constructed, with no use of a proper and qualified construction team. Albeit, the importance of having reliable constructions in a country that is affected by so many climate difficulties does not fade away.

Typically, several tests are already specified by international and national regulations in order to confirm the proper physical characteristics needed for each construction material. These tests range from chemical analysis to physical strength tests that are useful for analyzing behavior, yet all require altering the sample. X-ray techniques are famous for being non-destructive. Though it is not exactly new, it was mainly applied in the medical field before other uses were found. The ability to observe the sample through X-ray provides a much wider scope of information about the material and the state it is in. The debate on true porosity could be settled by application of micro computerized tomography (micro-CT) with sufficient resolution.

Mineralogical and chemical characterization can provide a wider view of the true composition of these building blocks and confirm if they are in line with the typical materials used and of the quality stated by the manufacturers.

1.1 PROBLEM STATEMENT

Ecuador is a volcanic region that is prone to various natural hazards, including seismic activity, volcanic eruptions, landslides, and floods, which all pose significant risks. To ensure stable and reliable constructions it is necessary to count with the security of good construction materials. Construction, in many cases, is done with no surveillance and/or guarantee, on any of the involved parts, that it will meet the minimum required characteristics to be considered safe. More so, it is common practice to use volcanic ash as a source of materials for construction, which does not necessarily meet the required standards for safe building. Evidence of wall deterioration within months of construction has been found in several structures across the country, particularly in mountain regions. This problem has also been reported in previous studies[1,2,3,4], where the main reason behind faulty structure behavior is related to the quality of the construction materials used, that might not necessarily comply with the established national composition standards. Several climate and overall geological factors also contribute to the damage of different buildings. This project focuses on the study of certain samples taken from the city of Ibarra, Ecuador, to determine the degree of the damage from haloclasty, and the relation it has with the construction materials chosen.

1.2 OBJECTIVES

1.2.1 General objective

Study of deterioration by haloclasty upon the most used construction materials in the city of Ibarra, Ecuador.

1.2.2 Specific objectives

- Identification of crystalline phases and location in construction samples through XRD.
- Analyze changes of porosity throughout the construction samples with micro-CT.
- Correlate the composition with the porosity and damage of different materials due to haloclasty.
- Deduce salt composition and mineralogical source of construction materials used.

2 THEORETICAL BACKGROUND

Ecuador is situated on the South-American plate and east to the boundary between the South-American and Nazca plate [5]. Seismic activity is common and intense mainly due to its location in a subduction zone between the Pacific plate and South American plate which is commonly known as the Ring of Fire [6]. The Ring of Fire has also been referred to as the Circum-Pacific belt, since it roughly surrounds the edges of the Pacific Ocean, and it is responsible for nearly 90% of earthquakes all around the world[7].

Since the Ring of Fire is mostly composed of a series of volcanoes, both above and below water, earthquakes are not the only risk to human life near the Ring. The eruption from volcanoes can spread ash made of minerals, rocks and volcanic glass. Either pyroclastic flow or volcanic debris are able to cause destruction in large scales [8]. One of the most devastating effects of volcanoes comes from lahars, these flows of sediments combined with water can reach up to hundreds of kilometers from the eruption at great speed and cause massive destruction[9]. Damage to infrastructure from volcanic eruption can come in a variety of forms: burial, ballistic impact, foundation failure, excessive wall or roof load, collapse, ignition, corrosion, etc. [10].

While it's true that volcanoes present many risk factors to adjacent communities, there are also advantages. Cinder and basalt from volcanic eruptions can be used as material for concrete[8].

According to local news, over 1,5 million Ecuadorians live in self-constructed homes that do not rely on government approval[11]. This makes them, in most cases, unsuited against natural disasters. Additionally, the informality that comes with these constructions normally leads to an excess of habitants per space, which increases damages on the property and surroundings, especially if there is not a proper connection of basic services; unproper drainage can cause serious detriment to the surrounding soil and weaken the foundations.

One of the most usual problems seen in houses all around the country is the excessive humidity in both interior and exterior sides of walls. Though repairs never surpass the cost of construction, the need for frequent repairs can become costly[4,12]. By paying attention to construction quality, these costs can be mitigated.

Due to all of that and more, it is of the utmost importance to select the correct materials for construction.

2.1 CONSTRUCTION MATERIALS

From building homes, offices, and even roads, the most sought out material for constructions is typically cement. Cement can further be combined into concrete, variations on cement serve as mortar for bricks. Along with other materials such as clay bricks, iron beams, glass and porcelain[13], they all aid, and at times, combine for aesthetic and functional purposes. This work goes in depth on particularly two different construction materials and furthermore, compares them: concrete and clay bricks.

2.1.1 Cement

It is a binding material that can be activated on hydration. Its composition depends on the type of cement, but in general cements contain calcium silicate, calcium sulfates and calcium, aluminum, ferric and silica oxides[14]. Cement is manufactured from limestones and clays, with a greater concentration of limestones than clay; the geological age of whatever source is used does not influence the outcome of the cement as much as the chemical composition. The amount of oxides, particularly magnesium oxide, is regulated to ensure correct mechanical behavior of the cement [15]. It is mainly used as a binding material since alone it would be too costly and it can deform after several wet-dry cycles[16].

Portland cement is a particular type of cement that is very popular worldwide due to its increased strength, versatility and durability. It is fabricated from clay or shale mixed with limestone or marl and burned at high temperatures; which is different from other types of cements[17]. It has up to 80% tricalcium and dicalcium silicate, which comes from the mix of lime, silica, alumina and ferric oxide[14] (though sometimes alumina is replaced with a higher iron content, and lime can be replaced to an extent by magnesia [17]).

2.1.2 Concrete

Concrete is one of the most versatile construction materials. It is made from cement, water and aggregates, and it is usually considered the cheapest of construction materials throughout the world since it is typically used to form the foundations of any building. Using concrete as the matrix of a composite is most beneficial to enhance certain physical properties depending on the particles or fibers added[14]. Since cement with water form a cement paste that stiffens overtime, physical properties of concrete vary throughout time. If there is an excess of water then drying time becomes slower and concrete takes longer to harden[18]. Usually, certain chemicals are added to the cement paste for different end goal consistencies that change the behavior of the final product[19]. The nature, proportion, placement, exposure conditions and quality of ingredients are all determining factors that influence concrete behavior[20].

The particle size of aggregates also has a fundamental contribution to physical properties. According to German nomenclature of grain size (DIN 4022, 1987)[19,21] the names of each particle size range are defined as shown in Table 1.

Table 1: Nomenclature of soil particle size distribution

Name	**particle size**
Clay	<0.002 mm
Silt	0.002 – 0.6 mm
Sand	0.6 – 2.0 mm
Gravel	2.0 – 60 mm
Stone	> 60mm

There are different types of concrete depending on the end use, but mainly they must all comply with certain standards of workability, durability, strength, air entrainment, shrinkage and creep, in order to be applied for a determined construction project.

2.1.3 Clay Brick

Clay bricks were very popular for construction long ago and to this day. Their composition can be as variable as concrete but mainly they have: sand, aggregates, clay and a binder; other additives could also be included like organic or latex additives, pigments, etc.[14]. Generally speaking, brick is a raw industrial material that starts from a soil and goes through the process of being blended, moistened, and even chemically modified to fit the required standards[18]. In the end, bricks vary a lot in composition and designs according to their application. Bricks can be classified by their production method or their characteristics. Some bricks are even designed with spaces to make the material more lightweight, improve on thermal properties and even reduce costs[22].

The main requirement is that the materials used to fabricate bricks must behave plastically when moistened so that it can fill a mold and then pass into a kiln to heat up and harden without cracking[18]. Yet, bricks can also be made by extrusion, and through this method they tend to be stronger and less porous[19]. The composition requires particles smaller than 53µm to obtain plasticity, combined with bigger particles up to 1168µm to control cracking, warping and shrinkage[23]. Bricks can be classified in three different groups: facing, commons and engineering bricks. Facing and engineering bricks tend to be of higher cost since they are made from higher quality clay and in the case of facing bricks, have higher demand to meet aesthetic requirements; commons are bricks of lower clay quality that are cheaper yet aren't necessarily as durable as the other two[18,19].

Mortar is a material that behaves plastic while it set but after a certain period of time it begins to harden. Since it is meant for filling gaps in order for the construction to resist air and water flow, it's made from a binder and a filler[14]. The composition varies as much as with bricks, but its function is similar to cement and sometimes even interchangeable to work with clay bricks. The overall strength of the construction not only depends on the brick and mortar but also the pattern in which the bricks are stacked.

2.1.4 Rock

Usually, rocks can fall into one of three categories, depending on their origins: Igneous, Sedimentary or Metamorphic. Igneous rocks form from the solidification of magma[24]. Sedimentary rocks are created by sedimentation of weathered rocks on the surface[25]. However, metamorphic rocks come from the reformation of an igneous, sedimentary or even another metamorphic rock that has been subjected to high temperatures, pressure and/or hot fluids with concentrated minerals. These factors cause the previous rock to change its mineral composition and become denser[26].

Rocks aren't usually used directly in construction. With exceptions like armourstone, which is picked from a quarry and transported to the shoreline with the sole purpose of distributing several different sizes of dense and durable rocks[27] that will protect against erosion, but with no significant processing of any kind. For construction, it's preferable to choose rocks that have mostly uniform cubic-like particles, that also comply with durability and strength standards[18].

2.2 PRODUCTION OF CONSTRUCTION MATERIALS IN ECUADOR

The construction sector in Ecuador has always been a significant contributor to the national Gross Domestic Product (GDP) and 100% of the cement demand in the country is covered by national production[28,29]. The private sector covers most constructions while the public sector covers the construction of streets, roads, etc[28].

When the mechanical behavior of concrete fails, it's plausible that it is due to the composition of the cement used and its quality. Constructions not only depend on the materials used but also, they must adequately foresee in the future what climatic characteristics might affect the infrastructure to see what materials are better suited for the task. Given the diversity of environments in Ecuador, the production of only a certain material to apply in all constructions might come at a high cost for several structures [30].

Regardless of their differences, all cement producers go through the same three stages: recollection of raw material, production of clinker, and final product cement. The raw material is crushed until all pieces are of about the same size, and then heated in an oven to obtain clinker. The clinker is the base material for cement production, so it is then put in a cement mill to finally be bagged and dispatched. Mainly, there are two different cements produced: gray cement and white cement. White cement is made from clinker mixed with gypsum and white limestone which are harder to find and therefore this cement is more expensive. While on the other hand, gray cement is a mix of clinker with gypsum, pozzolans, ash or slag in variable proportions to obtain a homogeneous powder [28].

2.2.1 Cement Plants in Ecuador

There are mainly three companies that make cement in Ecuador: Andean Union of Cements (UNACEM), National Union of Cement Plants (UCEM), and Holcim. Only UCEM is not entirely private and is also Ecuadorian, while the other two companies are private and foreign[29]. As for their distribution all over the country, Holcim is the company with most cement plants, including locations in Guayaquil, Quito, Latacunga, Cuenca, Manabí, Machala y Ambato[31]. UNACEM is mainly focused on Imbabura with a cement plant in Otavalo[32]. UCEM has two cement plants, one in Cañar and the other in Chimborazo[33], yet they distribute their production through several different commercial entities.

2.2.2 Cement regulations in Ecuador

According to the Ecuadorian Construction Norm (NEC), all construction materials have to abide certain standards that can vary depending on the construction goal. The quality of the materials is subjected to an assessment on behalf of the Ecuadorian Accreditation Organism (OAE) and should be fabricated under the Ecuadorian System of Quality Law. Imported materials are also tied to these same norms. These standards are specified in several documents from the Ecuadorian Normalization Institute (INEN), each one tailored for a particular material [34]. All cements are made from clinker, limestone, water or calcium sulfate, additives and air in the cases that apply; the compositions can vary given the end use of the cement and they are specified as follows.

Building Technological Standards (NTE) INEN 152

This document specifies requirements for eight types of Portland Cement (PC). Chemical composition standards can be seen simplified in Table 2.

Table 2: Guide to the maximum amount of silicate and oxides allowed in PC composition. Summarized from INEN 152-4 [35]

	Type of PC				
	I & IA	**II & IIA**	**III & IIIA**	**IV**	**V**
Aluminum oxide	-	6.0%	-	-	-
Ferric oxide	-	6.0%	-	6.5%	-
Magnesium oxide	6.0%	6.0%	6.0%	6.0%	6.0%
Tricalcium silicate	-	-	-	35%	-
Dicalcium silicate	-	-	-	40%	-
Tricalcium aluminate (C_3A)	-	8%	15%	7%	5%
Sulfur trioxide: If C_3A < 8%	3.0%	3.0%	3.5%	2.3%	2.3%
Or C_3A > 8%	3.5%		4.5%		
Insoluble Residue	0.75%	0.75%	0.75%	0.75%	0.75%

In the same document, specifications of mechanical behavior requirements are specified for each type of cement and the tests that can be made to assure the product complies with the norms [35]. There are several exceptions to the chemical composition, in particular when the properties of the cement need to be adjusted for special applications. Therefore, Table 2 is more a general guide than it is a limitation.

<u>Building Technological Standards (NTE) INEN 490</u>

Hydraulic cements are able to harden even under water; composite hydraulic cements (CHC) achieve hardening underwater by combining two or more types of cements, one of which is not Portland clinker nor Portland cement [36]. Composite Hydraulic cements are classified in: Composite hydraulic cement for general use, Type IS (blast furnace slag Portland cement), Type IP (Portland Pozzolana cement), Type IT (ternary composite cement). Their chemical composition standards are shown in Table 3.

Table 3: Guide to the maximum amount of chemical compounds in the CHC composition. Summarized from INEN 490 [37]

	Type of CHC		
	IS (<70), IT(P<S<70)	**IS (≥ 70), IT(S≥70)**	**IP, IT(P≥S)**
Magnesium oxide	-	-	6.0%
Sulfate	3.0%	4.0%	4.0%
Sulfide	2.0%	2.0%	-
Insoluble residue	1.0%	1.0%	-

Table 3 shows chemical requirements that apply to all cements with air incorporators. With the special case for amount of sulfate depending on the particular application of the cement. An extra requirement for the mixture of different types of cement is to pulverize the rock source to the size of grain desired in the final product and make sure that the different cements comply with the same size grain.

These are just some of the specifications for cement chemical composition in Ecuador. Not all norms contain indications for chemical composition, the focus tends to be on the physical parameters, the mechanical behavior and response of the material.

2.3 GEOLOGICAL CHALLENGES IN CONSTRUCTION

As mentioned before, the proximity of Ecuador to the Ring of Fire makes it prone to earthquakes and also must deal with damage from volcano eruptions. In the 2016 Muisne earthquake, buildings with a reinforced concrete (RC) frame were found to suffer greater damage than buildings with timber or bamboo inside their structure[38]. Most of this damage was attributed to the use of sea sand in construction, that led to high levels of corrosion of the steel reinforcements, yet bad design was also one of the main causes for the degree of destruction[39]. On the other hand, ruins from volcanic ash are far less researched compared to those caused by seismic events, yet they can still cause severe wreckage to infrastructure, among other health and economic risks[40]. Volcanic ash is considered the highest risk to buildings in the case of a volcanic eruption since of all the expelled particles, ash is small enough to travel further in the direction of the predominant winds. Loading of ash on top of roofs can be detrimental to buildings[41] but dissolved ash can release cations that form sulphate and halide salts, which in contact with water, can disperse and impermeabilize roads and increase fluvial erosion, or even cause corrosion damage[40]. These factors make it challenging to construct homes that are secure from geological hazards. Yet it is not the only damage that can come to buildings in the country.

One primary source of damage towards construction that isn't directly related to human activity nor natural disasters is weathering. Weathering is a phenomenon that gains its name due to the fact that it involves the action of weather upon rocks, or in this case, construction materials. It can be divided in two different processes that complement each other: mechanical and chemical weathering. Mechanical weathering is comprised of physical occurrences such as: freeze and thaw cycles, decrease in pression from overlying rocks, salt crystal formations, or cracking from plant roots. When mechanical weathering occurs, then fresh area of the rock is exposed and vulnerable to chemical weathering [25]. Chemical weathering is considered when there is a change of proportions in the original components of the rock due to chemical transformations [42]. These changes are usually more drastic in warm and wet climates since it has a high dependance on the presence of water, oxygen and carbon dioxide [25]. For both of these weathering processes, corrasion and rain play fundamental roles. Corrasion, also known as erosion by action of the wind, is effective as long as the wind can pick up abrasive particles that impact against a surface with enough force to cause damage at a micro scale, that can later grow into macro scale damage after continuous exposure. Particles between 100µm and 600µm are considered the ones that can cause most abrasion damage since they are light enough for the wind to carry, yet dense enough to cause a significant impact [43].

Much less mentioned is biological weathering. The presence of water can promote the generation of organisms that can interact with minerals and cause weathering effects on the surface. These organisms can be plants, microbes, and even fungi. Part of their metabolic activities interfere with the integrity of the structure of certain constructions due to their effect on minerals[44].

When soluble salts are found inside porous materials, they can lead to deterioration of said material. There are three key factors involved in the deterioration by weathering: environment, construction materials and salts [45]. More on the latter, salts can cause physical stress due to crystallization inside pores, differential thermal expansion, osmotic swelling of clays, hydration pressure and wet/dry cycles [46]. In particular, when submitted to water and heat, water acts as a solvent and carrier for several salts, while heat provides the necessary energy for several physical and chemical processes to accelerate the rate of damage [47]. This is the basis of damage caused by haloclasty, also referred to as salt weathering.

Under salt weathering conditions, moisture can be held for a longer period of time at the boundaries between two different types of rock, which can then cause the formation of salt crystals near the boundaries [46].

Origin of salts

As stated before, construction products such as cement, concrete and brick clay come from quarries that are filled with mostly limestones, gypsum or appropriate soil for clay. These rocks are made from minerals with mostly carbonate, sulphate and silicate salts, which eventually combine when making cement, concrete and other derived materials[48] (see Table 2 and Table 3). In the process of transforming raw material into a construction worthy substance, rocks mostly undergo fracture, sieving, heating and compaction. The chemical changes come from the process of adding certain admixtures that can provide the material of desired properties. Naturally, cement contains alkali sulfates, and, if not fired at the correct temperature it may contain sodium sulfate as well [49]. Sodium salts such as sodium chloride, sodium nitrate and sodium sulfate are typically associated with efflorescence, the latter being considered the most aggressive of all[50]; these salts come from groundwater or rainfall[48]. Salts can also originate by other external sources, such as air pollution, sea spray, interaction between other building materials or even from coatings that don't have the proper composition[51].

When rain hits a porous rock surface, different dissolved salts can fall into the pores. If the rate of evaporation is lower than the rate of salt migration, then salts could travel and recrystallize. Once salts migrate outwards, after a drying period, efflorescence can be spotted on the surface due to salt crystallization[46]. The mere presence of water can allow dissolution of salts already present in the material. In many ways, water can weaken the material by lowering mechanical resistance and cause efflorescence and subflourescence[43].

Pores

All materials contain pores. Their sizes, connectivity, distribution and form, become a determining factor in several chemical and physical processes and the overall characteristics of the material, like: thermal conductivity, durability, strength, density, etc [52–54]. Pores are defined as void space that is surrounded by walls [55]. They can be either closed and isolated or open and connected. In this sense, the connectivity between pores is fundamental for studies of diffusion of fluids throughout a material[49,53].

According to the International Union of Pure and Applied Chemistry (IUPAC), there are mainly three size classifications for pores: microporous, mesoporous and macroporous (Table 4) [54].

Table 4: Pore classification according to size.

Pore classification	Size range
Macropores	> 50 nm
Mesopores	2 nm - 50 nm
Micropores	< 2 nm

The width of a pore is not necessarily a good measurement since it highly depends on the shape; so, there is some leeway in the previous classification. Pore shapes often fall into one of three categories: cylindrical, ink-bottle shaped or funnel shaped; all of which can be open (Figure 1 a)) or closed (Figure 1 (b), (c), (d), (e) and (f))[54]. The shape and size are determined by the formation process of the material and the time and degree of exposure to external forces.

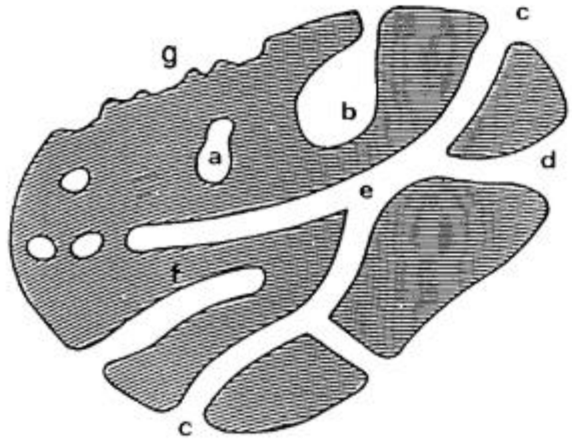

Figure 1: Different types of pores according to their shape. (a) small closed pore. (b) blind or dead-end pore with an ink bottle shape. (c) cylindrical open pore. (d) funnel shaped pore. (e) multiple open pore. (f)blind open cylindrical pore. (g) surface ruggedness that does not classify as a pore since it is not deeper than it is wide. Source: Technical Report published by the IUPAC [54]

Pores can also be characterized by their origin in primary and secondary porosity. Primary porosity is composed by all the spaces between grains when a material first settles. It is affected by the particle sizes, sorting, the compaction and degree of cementation[25]. In the case of cementitious materials in particular, these voids form due to the ratio between water and solid matter, the shape, size and surface texture of the particles, the raw materials used and the chemical admixtures, as well as the compaction and mixing method[56]. Secondary porosity, on the other hand, develops as time passes only after the material consolidates[25]; it can appear due to fractures or weathering.

Deterioration mechanism

The mere presence of salts is not enough to initiate deterioration upon natural or artificial materials. In order for salts to move throughout the pores they rely on water in either liquid or gaseous state [49]. One parameter that helps predict the transport mechanism is the moisture content, which is mostly dependent on porosity and pore size distribution. For salts to enter the pores of a structure, there are usually three sources, from the rise of groundwater, soaking from rain water or surface condensation.

There are many mechanisms that describe the transport of salts through a material. For salt crystallization to damage porous materials, the salt solution must be supersaturated to act as a driving force for the crystallization process. Salt damage can also be caused by surface scaling, deep cracking, expansion, granular disintegration, surface powdering and microcracking [57]. It is not only a matter of where the salts recrystallize, but also how they crystallize and what stress does that cause from within the structure [46] that defines damage done by haloclasty.

2.4 CHARACTERISTICS OF STUDY AREA: IBARRA CITY

San Miguel de Ibarra, known as Ibarra for short, is the capital of the Imbabura province. Located towards the northern part of the province, Ibarra lies at the foot of the Imbabura volcano. As the largest city in the province, it stretches to cover an area of 242.02 km^2 [58] where approximately 181.175 people live [59]. Sometimes, Ibarra is also called “The White City”, known for its mostly white houses that contrast with cobblestone roads[60].

The Decentralized Autonomous Government (GAD) of Imbabura states that Ibarra has mostly a semi-humid mesothermal equatorial climate that usually has a temperature variation between 10 and 20°C [61]. Ibarra is around 2225 m.a.s.l. and has an average precipitation of 1784 mm per year[62].

In addition to its climate and geographical features, Ibarra also has seismological considerations. For seismology studies, the determination of the Z factor is an essential indicator of seismic risk. This factor represents the maximum acceleration in rock expected for a designed seismic event and is presented as a fraction of the gravitational acceleration (g). Notably, Ibarra has a Z factor of 0.40, which falls within the high-risk zone for seismic movements, according to the Ecuadorian Norm for Construction [63].

3 METHODOLOGY

The methodology employed in this thesis aims to comprehensively investigate the porosity distribution, shapes, and sizes of thirty construction material samples that were divided into 4 different categories. By employing micro-CT imaging, this study delves into the intricate details of the internal structures of pores in each sample. The acquired data allows for a detailed analysis and subsequent comparison of the porosity characteristics among the different materials. To complement the obtained results, a modified variation of the Archimedes method was utilized for determining pore volume.

3.1 SAMPLE ACQUISITION

Thirty samples of several materials including: cobblestones, brick wall, concrete, slabs and lava rocks; were taken from the city of Ibarra on the 2nd of November of 2021. The locations were spread out throughout the city, taking samples specially of places where deterioration was visible due to the color difference on the same surface. Each sample was roughly the same diameter and with variable heights. Table 5 shows the construction material of each sample.

Table 5: Sample numbers according to the 4 categories of the studied construction materials

Material	Sample number
Lava rock	7, 12-16, 24-27
Brick	5, 6, 8, 9, 19
Cobblestone	1-4, 10, 11, 20-22
Concrete	17, 18, 23, 28-30

The samples were extracted with the use of an electrical drill. A hollow cylindrical bit was attached to the electrical drill and used for in situ extraction of cylindrical cores with about 25 mm in diameter and to a depth that varied according to each sample. The drill bit was lubricated with water and slowly lowered until a sufficient depth was reached. The process was similar to Stein and Sander's method [64] to obtain histological core samples with the difference that the drill was mobile in order to extract cores from different parts around the city (Figure 2).

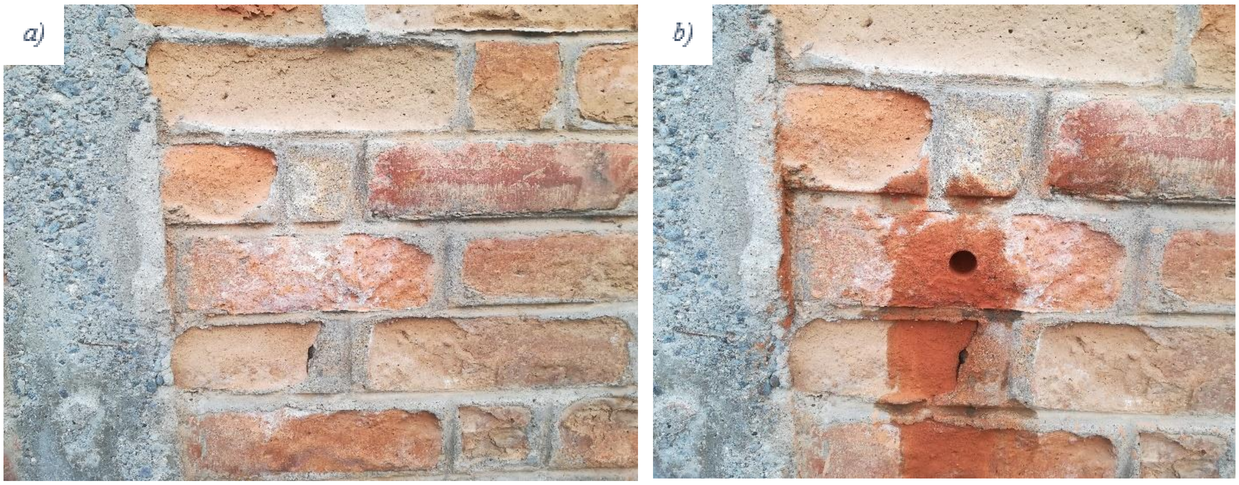

Figure 2: Example of an extraction site for a core sample. Picture of a brick wall with signs of weathering due to variation of colors on the bricks, particularly white spots that seem to indicate salt formation, and overall irregular shaped bricks that add a rugged texture to the wall. a) Before drilling. b) After drilling.

All cobblestone samples were made from concrete, but were treated as a separate material in order to compare and consider differences due to the use of concrete as a block or as a paving material. Samples 1 to 4 correspond to cobblestones, taken in different spots of the same cobblestone covering the outside and center of the stone. Samples 10, 11 and 22 are samples of different cobblestones that were squared unlike the first 4 cobblestones which had a unique cross-like shape. While, Sample 20 and 21 are also two samples of a cobblestone with discoloration towards the center.

Sample 17 was from a part of concrete used to cover the wall of a ravine. While, samples 18, 28, 29 and 30 are from concrete blocks from the grounds of a house.

Sample 5 and 6 are both bricks, the first one from a loose brick that had come off a wall and the latter was taken from a brick still in the wall. Samples 8 and 9 are other bricks from another part of the city. And sample 19 is one of the newest brick samples taken close to the park Ciudad Blanca.

All lava rock samples were taken nearby the city in two different sites. One site was in Quebrada Seca where samples 7, 12, 13, 14, 15 and 16 were taken. The other site was in the river Jatunyacu, where samples 24, 25, 26 and 27 were taken.

3.2 RECONSTRUCTION OF SAMPLE CORES

Each core sample was put inside the Bruker Skyscan 2211 micro-CT Scanner with a tungsten target. The scanner can detect down to 100nm, though resolution of samples were of 20µm. Voltage, current, exposure time and rotation step used for each sample measurement is detailed in Annex 1.

Parameters such as postalignment, smoothing, ring artifact reduction, and beam hardening correction were adjusted by trial and error through the NRecon software (Annex 2):

- Postalignment was not necessary to adjust in most cases. It helps when the images from the scan are blurred due to movement in the sample chamber while the analysis occurs, but since the scans were pretty quick then point drifting was not a significant issue to correct.
- The smoothing parameter allows the reduction of noise but with the cost of resolution, in that sense, no sample was smoothed over a value of 10.
- Ring artifacts relate to the appearance of concentric circles inside the volume that is scanned. This can create issues when processing the image and detecting gray scale correctly. The problem arises due to a faulty detector element behavior, that can happen because of a change in temperature while the analysis occurs, beam-hardening, or any other hardware related problems [65]. To correct this, NRecon software allows the input of a value between 1 and 20.
- Beam hardening is an artifact related to the effect of polychromatic x-rays on the sample. Since the source of x-rays in the Bruker 2211 is not monochromatic, rather it contains a range from 20 to 190kV[66], the material that is analyzed tends to absorb low energy x-rays creating a high energy photon environment that reflects upon reconstruction[67]. Therefore, beam hardening filters can correct this attenuation factor.

Reconstructed images were verified through CTvox for an appropriate resolution (Figure 3).

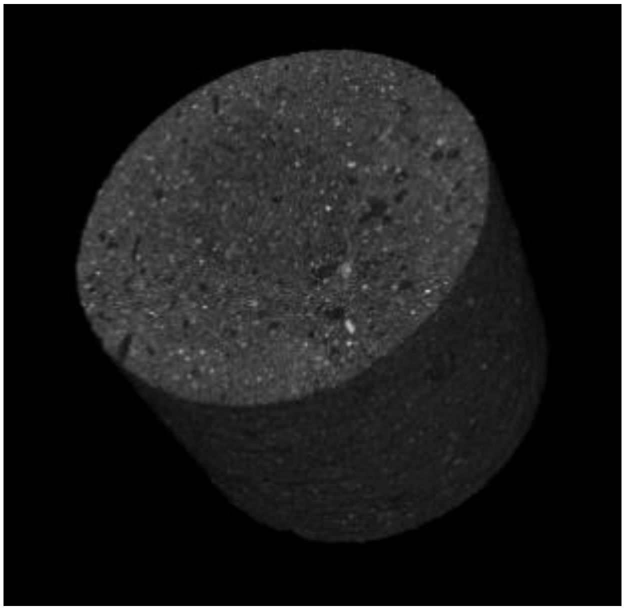

Figure 3: Reconstructed core of sample 8, a clay brick, viewed in CTvox.

3.3 Porosity analysis

The main focus was to analyze porosity in core samples with micro-CT. This method provided a detailed amount of information on each pore individually and overall porosity information of each sample. The overall porosity results were compared with the Archimedes method for determining porosity by calculating the pore density with distilled water. Each method is described in detail in the following sections.

3.3.1 Porosity analysis by micro-CT

Each sample had to undergo different processing. Thresholding, filters and despekle were different operations applied to each sample according to the resolution needed to distinguish pores from the material core. CTan software was used to make calculations on the reconstruction of the different samples.

Since all samples are cylindric with a similar diameter, a round region of interest (ROI) of 20.00 mm in diameter was chosen for all calculations, with which a volume of interest (VOI) was extended from the surface of the sample to the bottom. Samples were separated by material and analyzed by groups. Filtering, threshold and despekle was done to each sample through observation, trial and error. Most samples required an anisotropic diffusion filter which adjusted the noise well enough to apply a proper threshold for analysis (see Figure 4); the remaining brick samples required a median filter for the same purpose. After filtering and applying a gray threshold, a sweep despekle was applied in order to eliminate all but the largest object and further reduce noise. A proper 3D analysis allowed the reconstruction of volumes inside the region of interest, with a depiction of the structure and its pores. These 3D structures were then visualized with CTvox (Figure 5), highlighting, when possible, the connected pores and distinguishing them from all closed pores.

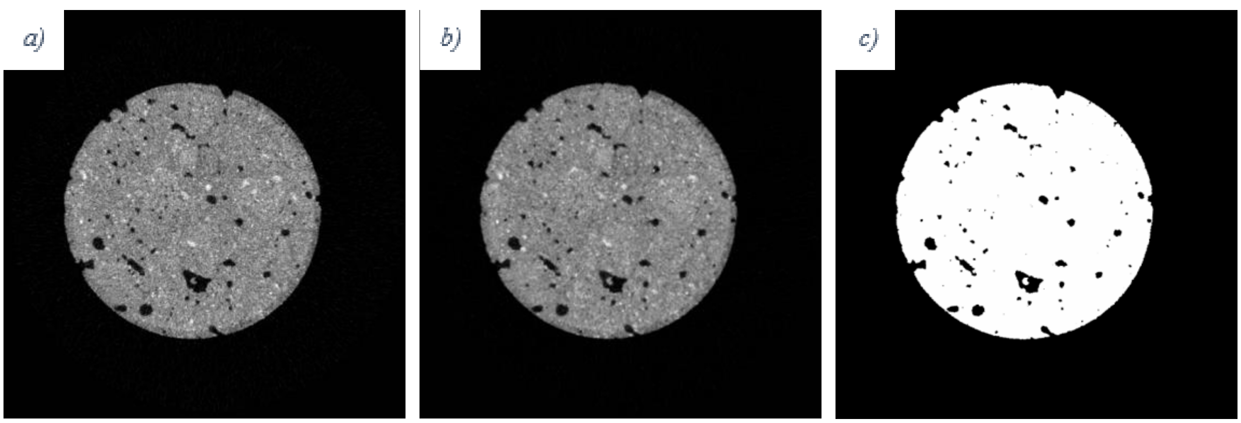

Figure 4: Effect of operations in CTan. a) Sample without filter. b) Sample after filtering. c) Distinction of matrix without pores after applying a threshold and despekle.

An individual 3D analysis was run for the pores of each sample in order to obtain information on the volume, surface, diameter, connectivity, and position of each pore as a separate object. The output file was analyzed in Excel in order to compare pore distributions along each sample in the Z direction. The volume along the Z axis was viewed as a sum of all pores for a given value of Z.

Just as the amount of pores was seen in the same way along the Z axis. Additionally, sphericity was analyzed in relation to the volume of pores and their position along the Z axis.

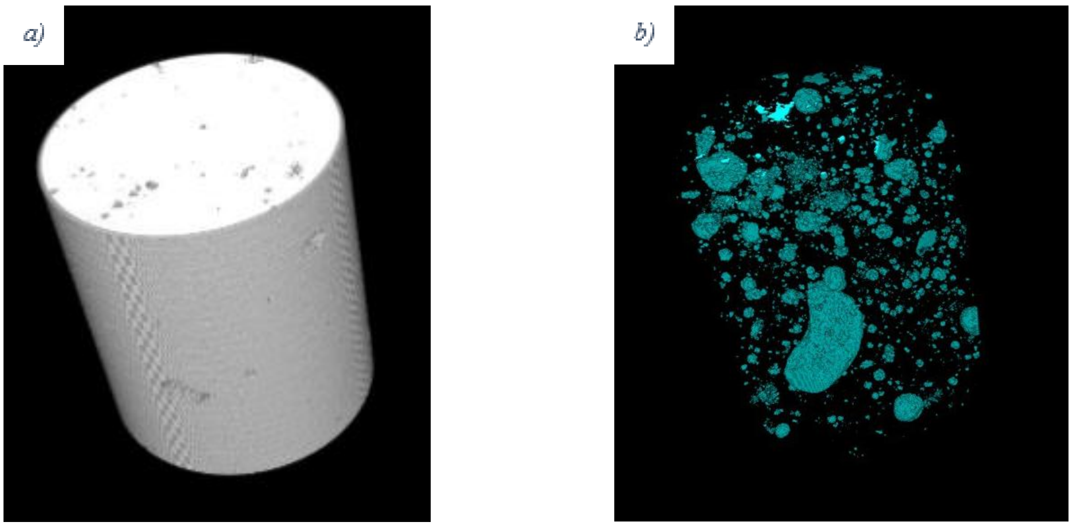

Figure 5: View of VOI in CTvox. a) Matrix inside VOI. b) Pores inside VOI.

3.3.2 Porosity analysis by a modified Archimedes method

To compare results from the computerized tomography analysis, 14 samples were weighed in a precision balance and soaked in distilled water, at 21°C, in a beaker with enough water to cover each sample (Figure 6). Initial and final volume was written down and the difference was considered as the volume of the sample. The volume was also calculated by averaging the diameter and height measurements and considering each sample a perfect cylinder, following the formula for volume of a cylinder shown below.

$$V_c = 2\pi r^2 h$$

Height and diameter of each sample was measured with an electronic vernier calliper at several points of the sample to obtain an average. After 3 days of soaking in water, each sample was taken out and lightly dried on all sides before weighing. The difference in weight between the wet sample and the dry sample gave an estimate of the open pores and water uptake of each sample. The mass difference was divided by the average volume to determine the porosity density which was transformed into a porosity percentage by using the density of water at room temperature as a conversion factor.

Figure 6: Sample submerged in a 100mL beaker for determination of porosity through Archimedes method.

4 RESULTS

From the data obtained after a 3D analysis of each core, porosity was calculated as the volume remaining from subtracting the reconstructed core from the VOI. This porosity was initially compared with the porosity calculated from the Archimedes method. In the following sections, a more detailed analysis is given for each construction material category. Finally, shape and sizes of pores are discussed for all categories and compared to each other.

Due to a problem of insufficient resolution, sample 23 was left out of all analysis. Samples 10 and 11 presented the same problem for an individual pore analysis but an approximation on total porosity was made.

4.1 POROSITY METHODS COMPARED

Through micro-CT analysis, a threshold was established to differentiate the pores from the matrix of each sample. The accuracy of this method heavily relies on the resolution of the images, which is why some samples could not be correctly analyzed.

On the other hand, the modified method of Archimedes has been used many times to measure apparent porosity, which includes interconnected pores. This method is particularly useful as a way to determine permeability. The errors from using this method are related to the appreciation of the measurement equipment and also the irregularity of the samples.

A comparison of both methods is shown in Table 6. For all samples except sample 14, the porosity determined by Archimedes method was higher. One important distinction to make is that the Archimedes method used the entire sample, while porosity for all samples determined by micro-CT was calculated only in a specific volume of interest (VOI), which was smaller and located towards the center of the sample. The reason why the entire volume of the sample was not taken into account for micro-CT is because pores that are towards the edges are influenced by the extraction process of the core. Also, the images for the reconstruction of the cores were not taken immediately after the extraction of the samples, so, pores that are inherent of the material might be confused with those that were created after the extraction, not only due to the extraction process itself, but also because of improper handling and storage. To avoid misrepresentation of porosity of each material, that could have been formed after extraction or during the extraction process instead of being inherent to the original material porosity, the analysis was limited to a VOI that excluded the exterior sides of the sample.

Table 6: Comparison of porosity percentage by micro-CT method and Archimedes method, including the percentage of connected pores.

	Sample	**Micro CT method**		**Archimedes method**	**Difference between methods**
		Porosity%	**Connected Pores %**	**Water Porosity%**	
Lava Rock	**7**	0.187	0.049	19.29(9)	19.107
	14	5.583	4.714	5.44(6)	0.145
	15	5.0763	3.881	10.1(2)	4.985
	24	0.654	0.453	12.1(3)	11.387
	25	4.181	3.831	9.98(3)	5.800
	27	0.52	0.476	14.32(7)	13.797
Brick	**5**	2.742	0.924	43.6(9)	40.912
	19	0.156	0.077	23.43(7)	23.273
Cobblestone	**1**	4.551	3.005	14.54(3)	9.987
	10	7.982	4.862	22.5(2)	14.567
	21	8.219	5.748	16.30(2)	8.087
	22	6.449	4.417	13.58(5)	7.128
Concrete	**17**	5.524	3.715	18.9(5)	13.416
	18	3.157	2.333	14.35(3)	11.195

The lava samples not only proved to have lower porosity in most cases, but also showed less difference with the porosity obtained in both methods. The highest difference was observed in the brick sample, which in part is also attributed to a lack of resolution in these samples. In particular, sample 5 showed the highest difference between Archimedes method and micro-CT. This was due to a particularly big pore towards the outside of the sample that was not taken into account. This also confirms the particularity of clay samples having a lower compressive strength than concrete.

4.2 LAVA ROCK

In general, lava rock samples displayed some of the lowest porosities and also the least variation between porosity calculated through both methods described previously (Table 6). Of all 10 lava rock samples, samples 7, 12, 13, 24 and 27 presented the lowest amount of porosity (Figure 7). On the other hand, sample 25 showed the highest porosity from all lava samples.

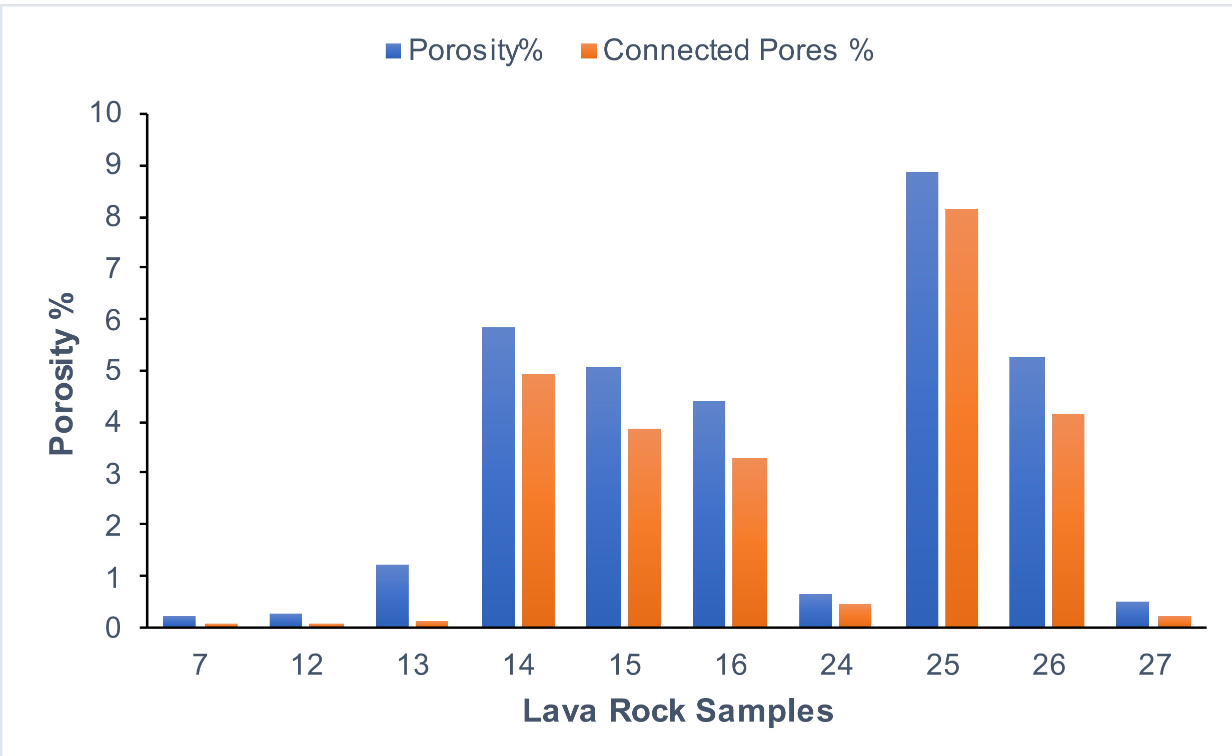

Figure 7: Percentage of porosity inside the VOI of the 10 lava rock samples. Total porosity is shown in blue, while only the connected pores are shown in orange.

Taking a closer look to sample 7, (Figure 8 a)) a polished cross section is depicted, in which no significant pores are distinguished. By looking at the sample under a 5x lens (Figure 8 b)) a few small pores between 30 and 120 µm in their mayor diameter can be seen surrounded by yellowish crystals. This seems to indicate a sort of weak point in the structure, since these crystals are not observed without a pore, or more, generally towards the center. This particularly is a sign that these pores might have formed due to the formation and evaporation of crystals, especially given their irregular shape. Under the same resolution, sample 25 (Figure 9 b)) shows a difference in pore size that varies significantly from sample 7. Pores from sample 25 are seen in a range of 70 to 420 µm in diameter.

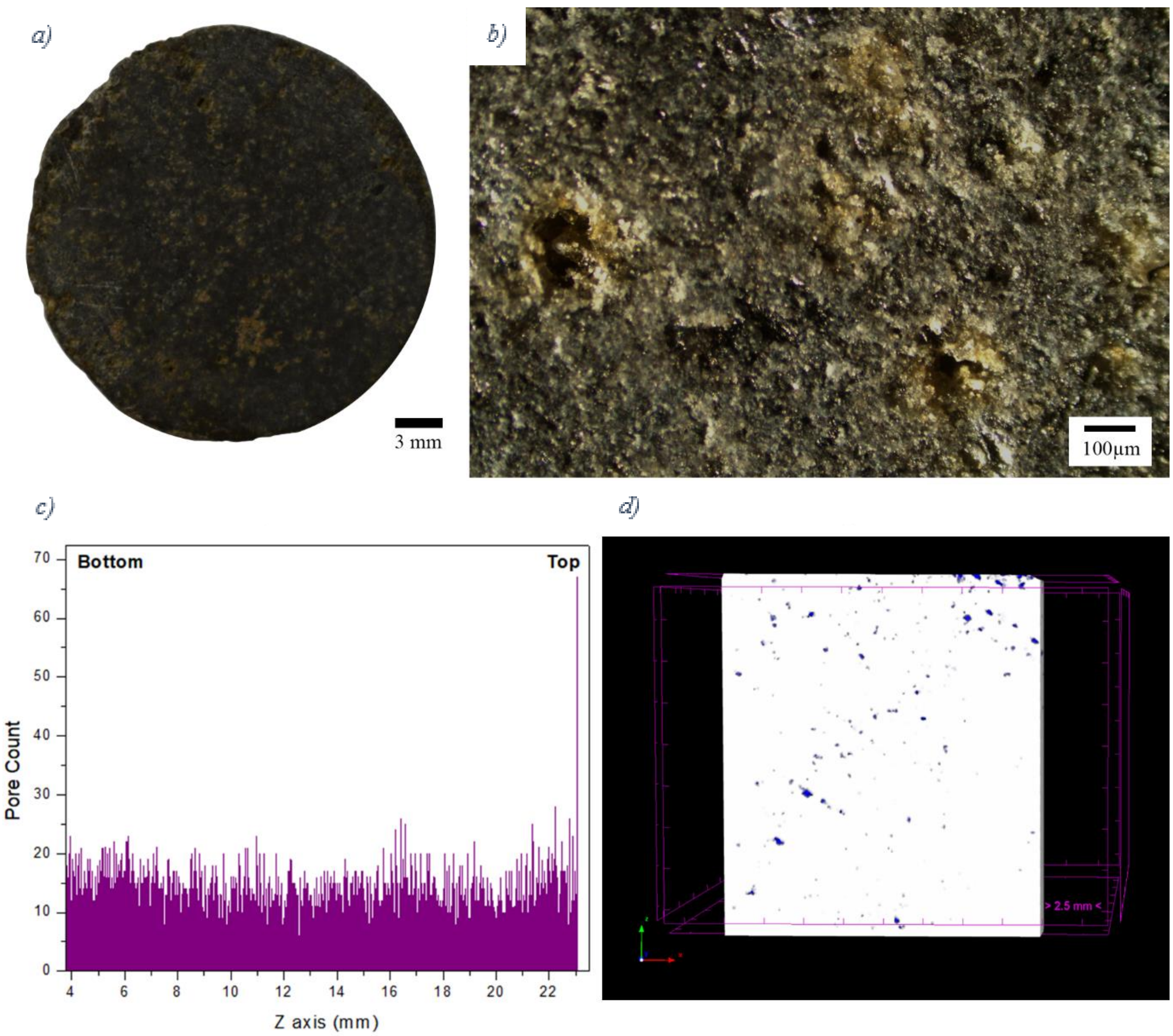

Figure 8: Different views of Sample 7. a) circular view of an interior side of the sample. b) view of the sample under a 5x increment lens. c) graph of the amount of pores along the Z axis. Top (surface) and bottom of the sample are indicated in bold letters. d) reconstructed sample in CTvox. Pores are highlighted in blue.

When comparing the amount of pores along the Z axis of samples 7 and 25, as the samples with lowest and highest amount of pores respectively (Figure 8 c) and Figure 9 c)). There is a tendency in which the surface has the most amount of pores and decreases significantly further into the sample. The average of pores in a cross section inside the VOI for sample 7 once past the surface is around 20 while for sample 25 the average is 30. These numbers aren't overwhelmingly different but they do support the fact that sample 25 has a higher porosity. What is significantly different is the amount of pores at the surface of each sample. Sample 7 came up to 67 pores on the surface cross section but sample 25 had a pore count of 149. While sample 7 seems to be denser and more homogenous, sample 25 clearly has quartz incrustations of different sizes which contributes to the formation of pores between the grains.

All reconstructed samples were observed in CTvox along different cross sections. In the case of samples 7 and 25 there was noticeably a difference in pore sizes (Figure 8 d) and Figure 9 d)). In the case of sample 7, the pores seem to get smaller towards the bottom of the sample. While in sample 25 a tendency isn't as clear.

Despite the evidence of more porosity in sample 25, the sample shows no unrefusable sign that pores were made from haloclasty. On the exterior surface side there is a larger number of pores but it does not account for the largest pore value. Furthermore, pores that were observed in sample 25 seem to have formed due to trapped gases and different sized grains instead of salt crystallization being the driving force for their formation. Sample 7 on the other hand does show signs of haloclasty, which establishes a precedent on how this phenomenon can affect somewhat similar rocks, from the same class, in diverse ways. It's natural to defend that this difference might only be enhanced when comparing materials from different sources.

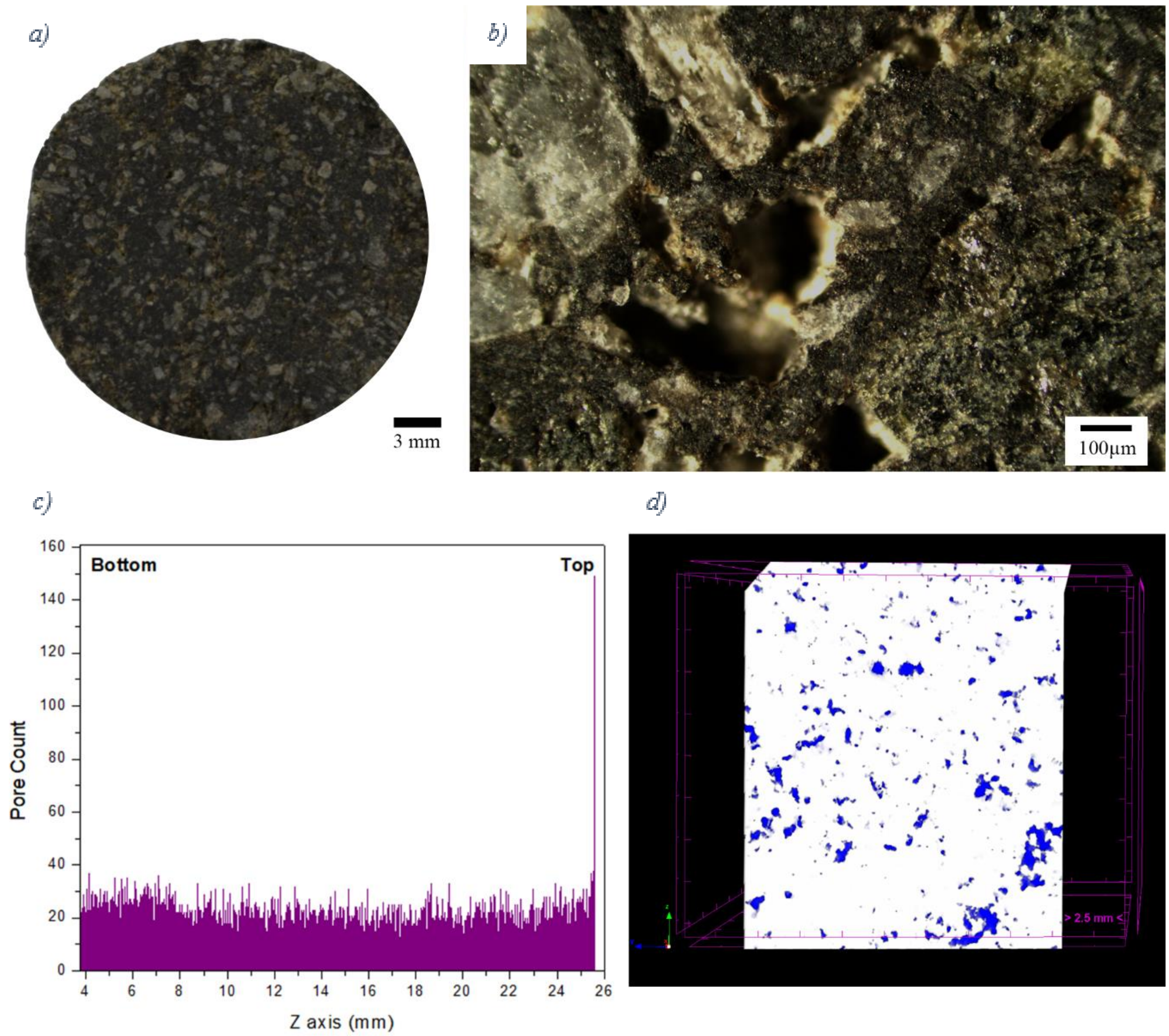

Figure 9: Different views of Sample 25. a) circular view of an interior side of the sample. b) view of the sample under a 5x increment lens. c) graph of the amount of pores along the Z axis. Top (surface) and bottom of the sample are indicated in bold letters. d) reconstructed sample in CTvox. Pores are highlighted in blue.

To get a better picture, the volume of all pores was graphed against the position throughout the Z axis. The total volume of pores of sample 7 seems to increase while closer to the surface (Figure 10 a)). This confirms the origin of these pores due to haloclasty and other external effects of the environment. In the case of sample 25 the highest value of volume isn't exactly at the surface of the sample (Figure 10 b)). This could indicate a migration of pores from the surface, or rather a deeper effect of haloclasty, if not the fact that the pores are unrelated to haloclasty altogether.

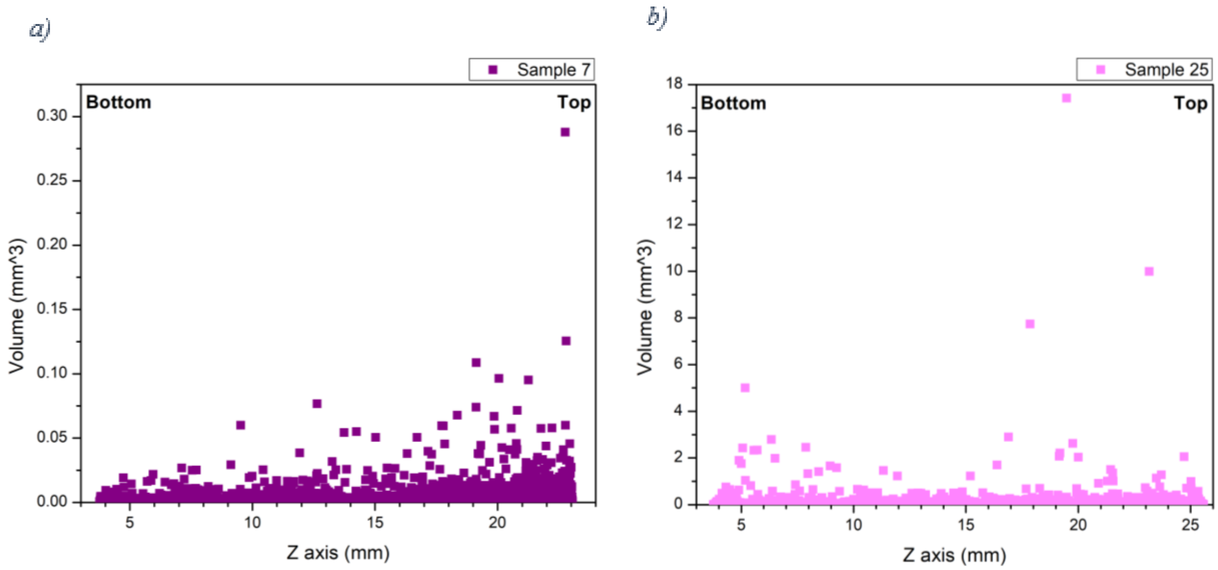

Figure 10: Volume of all pores from the interior of the sample to the surface. Top and bottom of the sample are indicated in bold letters. a) Total volume of pores of sample 7 along Z axis. b) Total volume of pores of sample 25 along Z axis.

It's important to consider that igneous and metamorphic rocks tend to have the lowest porosity since they form under great pressures, so most of their porosity is only secondary[25]. As both lava samples showed a higher number of pores towards the surface this supports the evidence of the pores forming after the formation of the rock.

4.3 BRICK

Brick samples seemed banded along a longitudinal plane. A visible discoloration was observed from a darker orange towards the top of the sample, to a more faded light orange towards the inner side of the wall. By the appearance of the state of the wall from which samples 5, 6, 8 and 9 were taken (Figure 11), it's most likely that they are common bricks made from low-quality clay. Yet, the porosity found in these samples was surprisingly low (Figure 12), due to the fact that bricks are made mostly from clay, which is a fine particle. The damage observed in the brick walls may be more related to the impurities of the clay from which the bricks were made, than the porosity.

Figure 11: Sites for brick sample extraction. a) Sample 5 belonged to a loose brick on the ground that showed visible deterioration due to the deviation of its shape from a rectangle block. b) Sample 6 was taken from the lower half of a brick wall with severe signs of damage and crumbling. c) Sample 8 comes from a brick wall with variation of orange tones and white spots where crystals effloresce. d) Sample 9 was part of a less visibly deteriorated brick wall but also shows slight variation of orange tones. e) Sample 19 was obtained from a more recent brick sample with barely any sign of physical weathering.

The sample with the lowest porosity was sample 19, which was also the youngest sample of clay bricks taken. Conversely, sample 5 showed the highest porosity. The Archimedes method for porosity determination varied a lot with brick samples in particular, yet the method agrees in sample 5 having a higher porosity (Table 6).

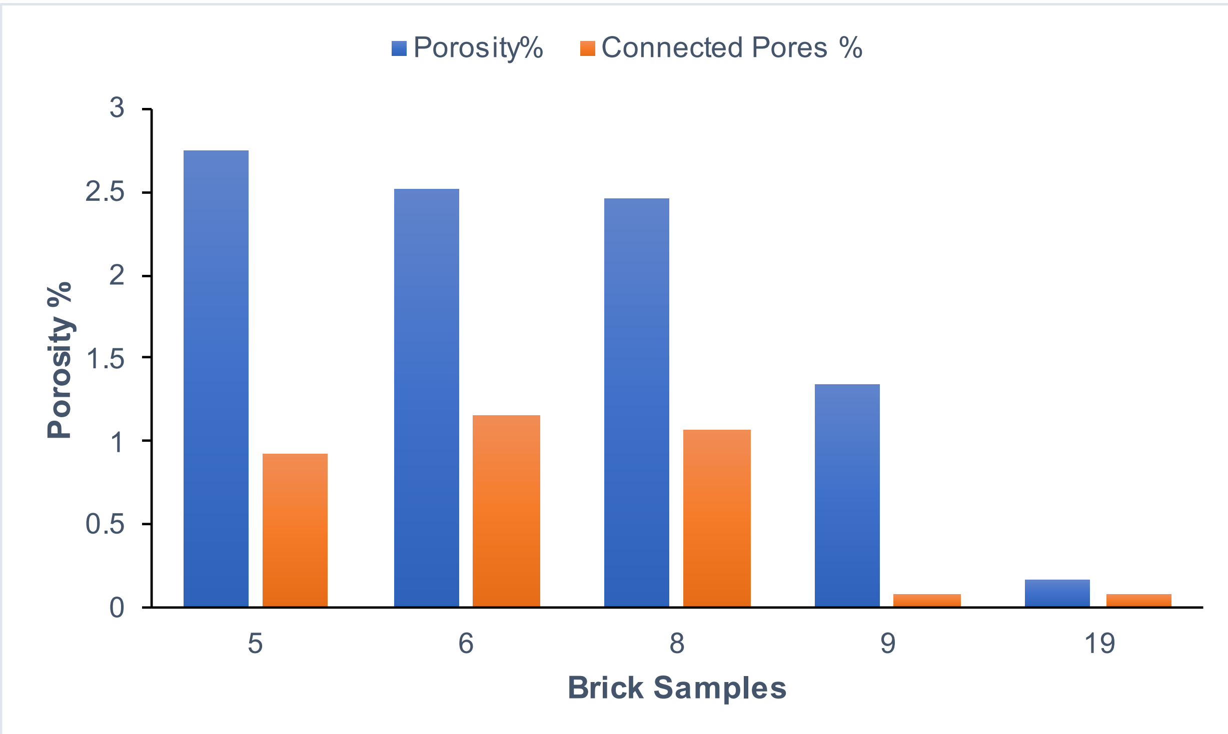

Figure 12: Percentage of porosity inside the VOI of the 5 brick samples taken (see Figure 11). Total porosity is shown in blue, while only the connected pores are shown in orange.

At plain sight no pores can be seen on the surface of sample 19 (Figure 13 a)), yet the amplified image of the sample shows relatively shallow pores that range from 5 µm to 260 µm (Figure 13 b)). Many small pores are seen on top of the darker areas of the sample, and the biggest pores seem to form besides larger particles. This was also confirmed while observing the reconstructed sample in CTan. Unlike lava samples, the majority of pores aren't on the surface of the sample in the case of brick 19 (Figure 13 c)). The resolution of the reconstruction was not enough to determine pores under 20 µm, but from the amplified image it is clear that there are several pores under the resolution limit. The view of the cross section doesn't show many pores and it would seem that the sample is rather dense, but it is also due to a lack of resolution (Figure 13 d)).

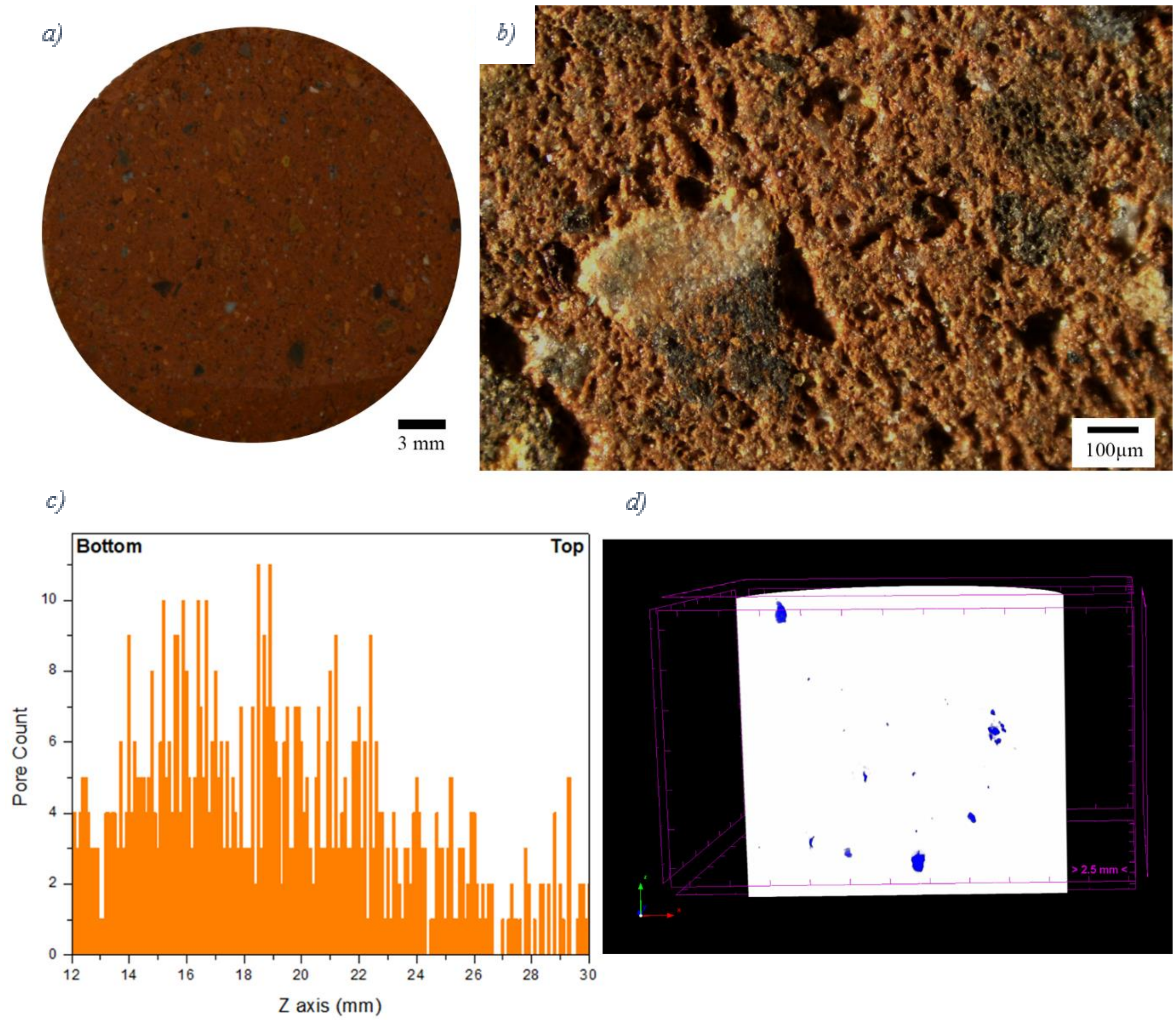

Figure 13: Different views of Sample 19. a) circular view of an interior side of the sample. b) view of the sample under a 5x increment lens. c) graph of the amount of pores along the Z axis. Top (surface) and bottom of the sample are indicated in bold letters. d) reconstructed sample in CTvox. Pores are highlighted in blue.

When comparing the volume of brick samples along the Z axis (Figure 14), in general, there is no particular tendency of the volume throughout the sample. Clay brick samples are more homogenous, thus causing less variation in pore size. In particular, samples 5 and 9 show higher volumes towards the surface of the sample, which is an expected sign of weathering by haloclasty. Sample 19 remains the sample with lowest porosity and the cross section with highest volume is shifted towards the bottom of the sample rather than the surface.

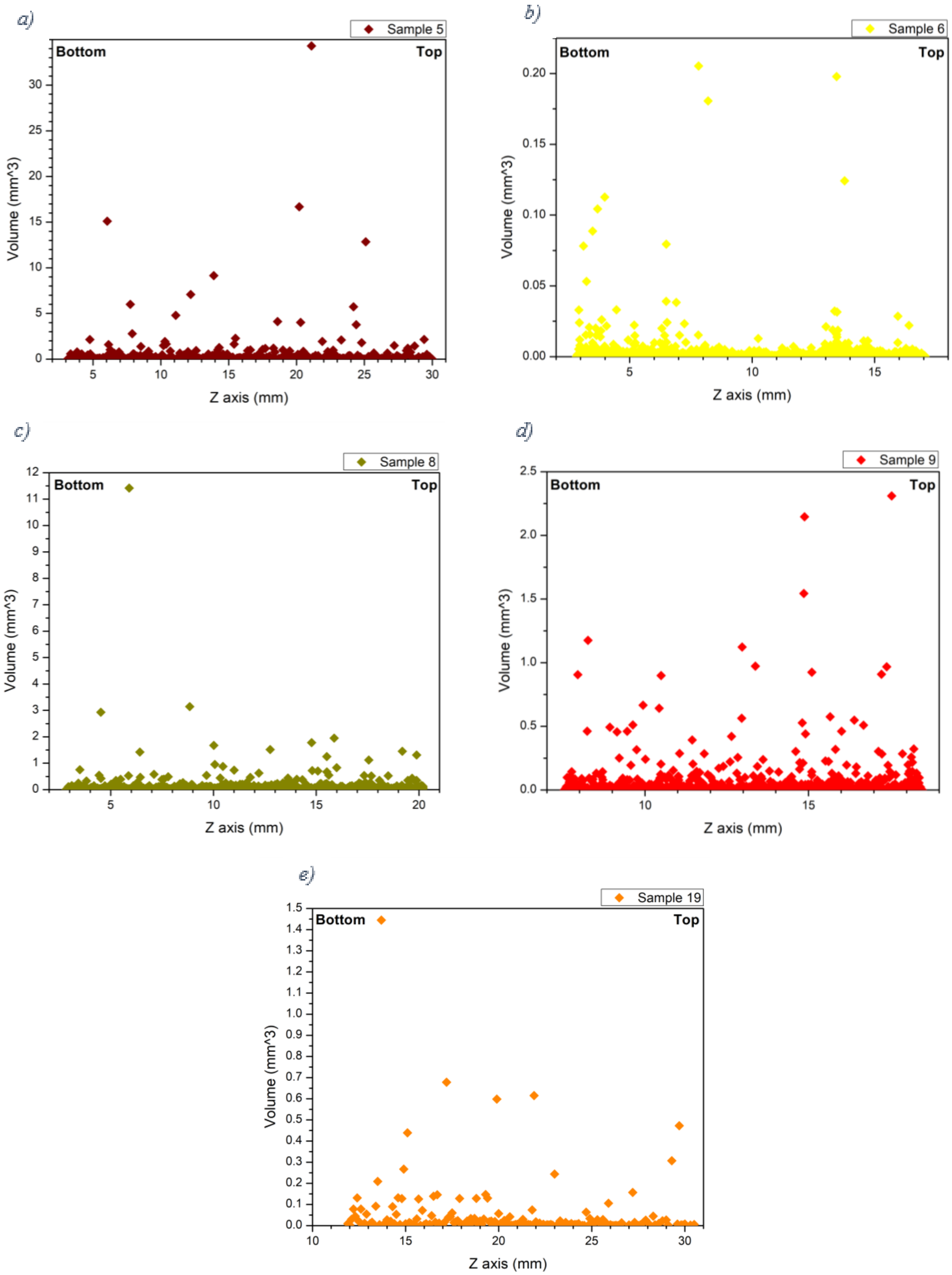

Figure 14: Pore volume longitudinal profile of clay bricks. Bottom and top of samples are indicated in bold letters. a)-e) Sum of pore volume along the Z axis for samples 5, 6, 8, 9 and 19.

4.4 COBBLESTONE

Samples 10 and 11 showed the highest porosity even though, as mentioned before, the resolution was too low to do an accurate analysis on individual pores (Figure 15).

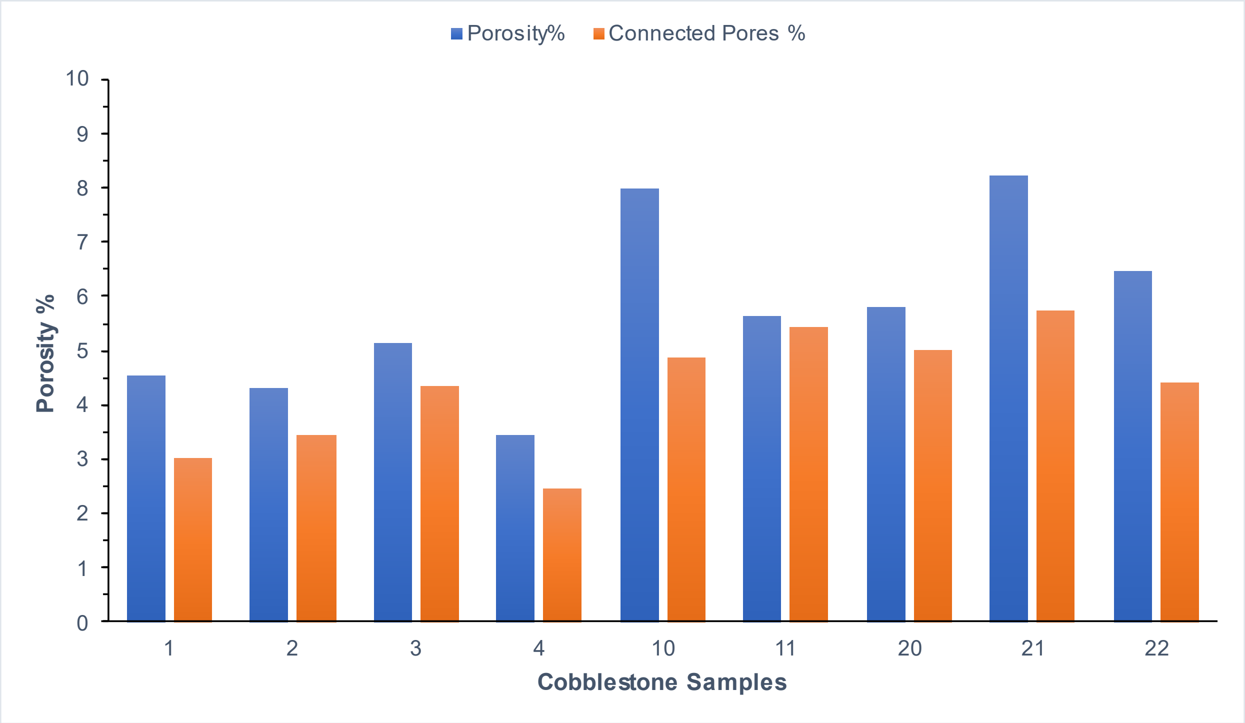

Figure 15: Percentage of porosity inside the VOI of the 9 cobblestone samples. Total porosity is shown in blue, while only the connected pores are shown in orange. Samples 10 and 11 show approximated values due to the resolution problem with micro-CT. The extraction site for cobblestone samples 1-4 is shown in Figure 16 a) and b), while samples 20 and 21 are seen in Figure 17 a).

Samples 1 to 4 are all from different zones of a same type of cobblestone (Figure 16 a) and b)). It would seem that the center is the zone of most damage, which was where sample 4 was taken. But, sample 4 has the lowest porosity according to the calculations with micro-CT (Figure 15).

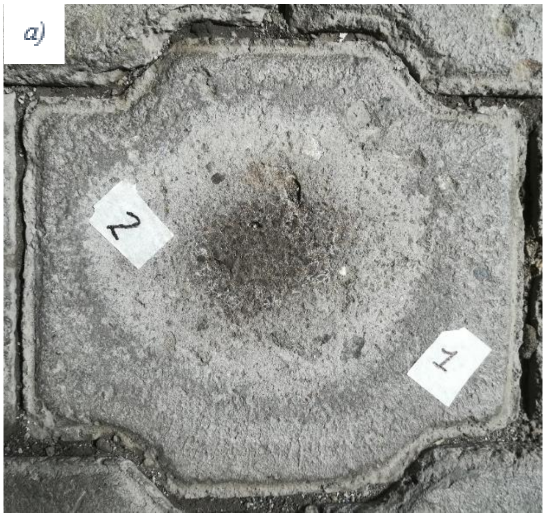

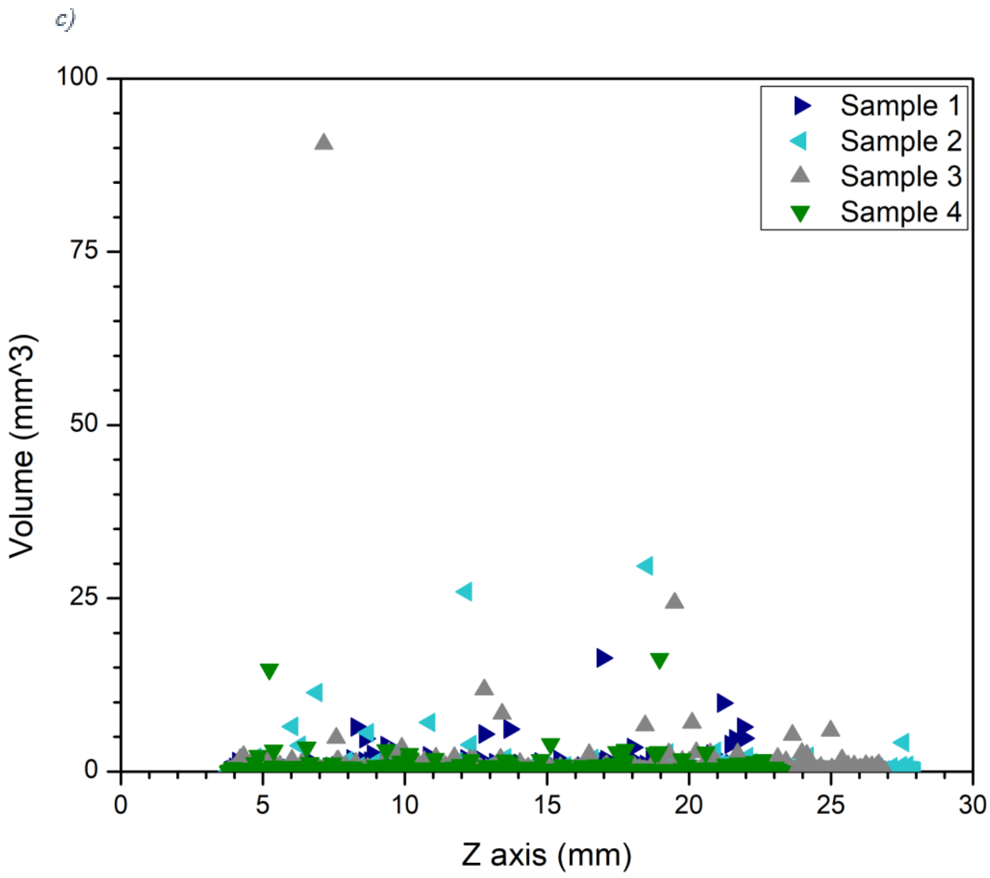

Figure 16: Analysis of volume of pores in samples 1-4. a) Extraction site of samples 1 and 2. b) Extraction site for samples 3 and 4. c) Total pore volume along the Z axis of cobblestone samples 1-4.

It’s interesting to see how the samples that have the largest volumen at a given value of Z near the most inner side of each core are samples 3 and sample 20 respectively (Figure 16 c) and Figure 17 b)).

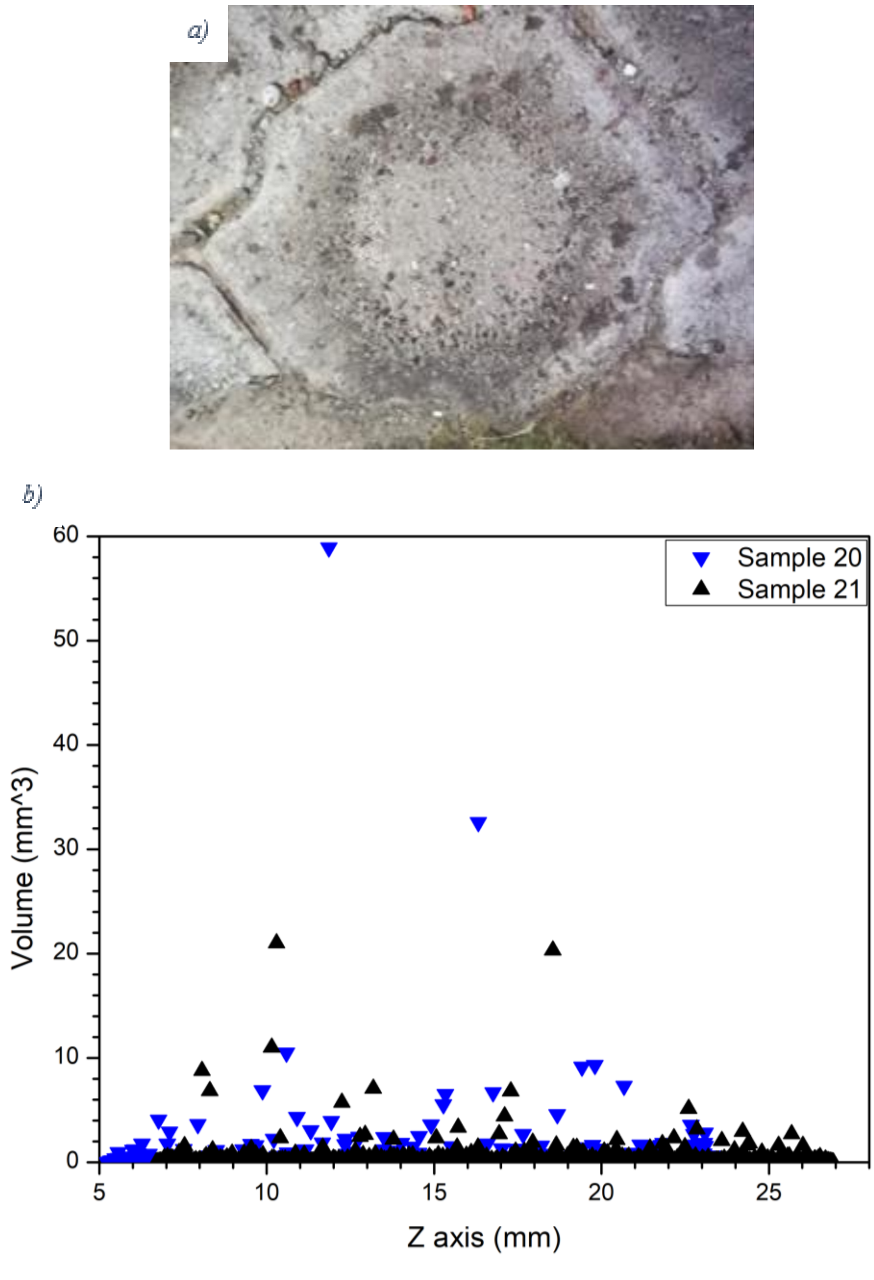

Figure 17: Analysis of pores of samples 20 and 21. a) Sample 20 was taken from the center of the cobblestone. Sample 21 was from the outer ring. b) Total pore volume along the Z axis of samples 20 and 21.

Recalling the pattern observed in the cobblestones, samples 1 to 4 were taken from different colored parts of a cobblestone that was darker in the center and had a light colored ring that did not equal the color towards the edges; samples 20 and 21 on the other hand were taken from a cobblestone with the opposite color scheme, the center was a light color surrounded by a darker colored ring. Sample 3 corresponds to the light colored ring while sample 20 corresponds to the light colored center.

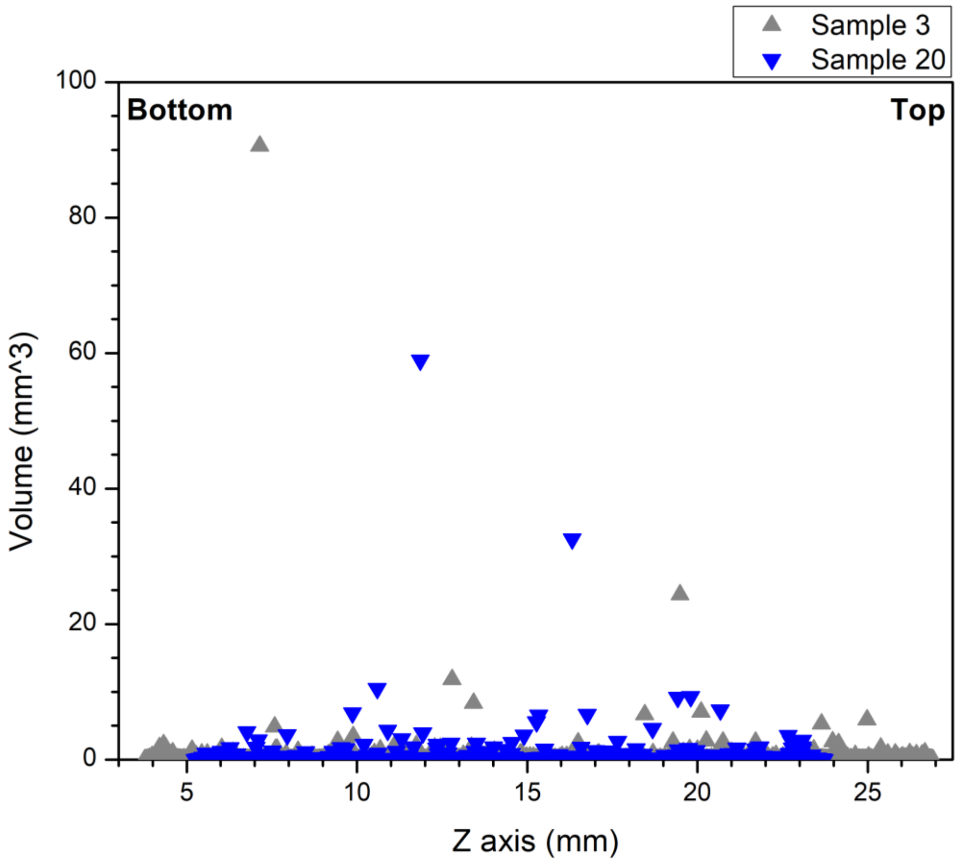

Figure 18: Comparison of total pore volume in samples 3 and 20. Top and bottom of samples are indicated in bold letters.

Considering that the samples differ in size and time since they were placed, they seem to share a tendency to be more hollow the deeper it goes (Figure 18). On the other side, the darker areas in both cobblestones would be represented by samples 4 and 21 (Figure 19). Though not identical, these samples also share similarities, with the important distinction that sample 21 has a higher pore volume than sample 4. Due to the appearance of sample 4, it would seem that it is the most damaged zone yet the porosity analysis shows that it has lower porosity than the other cobblestone samples. This is important when relating degree of damage to porosity. Though most damage occurs in more porous materials, damage isn't represented completely by the amouth of pores in each sample.

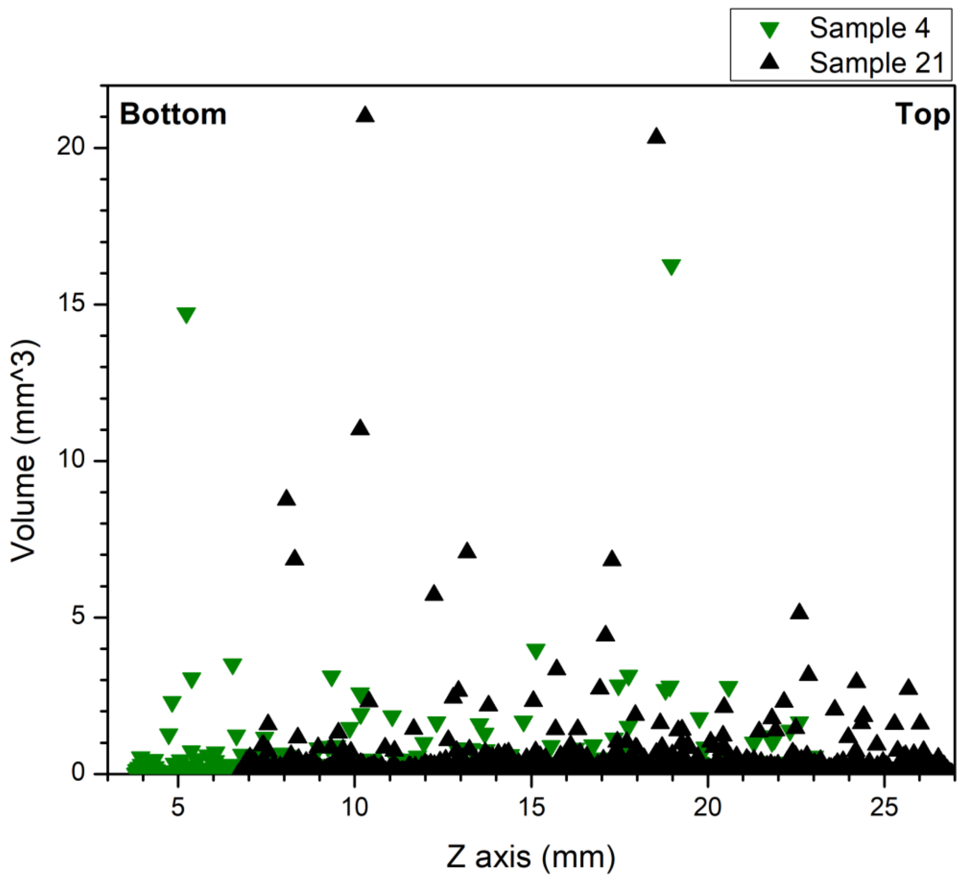

Figure 19: Comparison of samples 4 (green triangle) and 21 (black triangle). The top and bottom of the samples are indicated in bold letters.

When considering the pore distribution of these sample, for the first four cobblestone samples (Figure 20), a general tendency of pores in samples 1 and 2 is shared. Sample 2 shows a higher percentage of pores than sample 1 in a range of 0.50 mm midpoint. While the larger pores get there are fewer of them in total. Samples 3 and 4 were closer to the center of the cobblestone and though sample 3, in particular, showed pores of a larger diameter than sample 4 which was taken from the center of the cobblestone, sample 4 shows a higher percentage of pores that are wider.

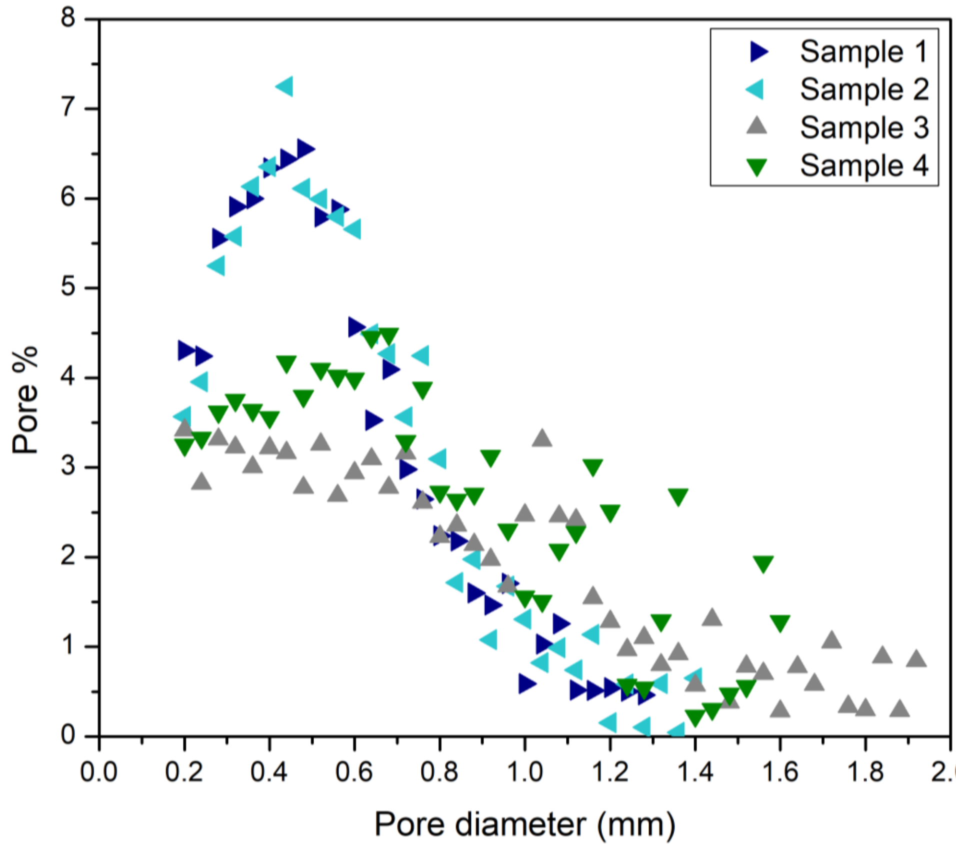

Figure 20: Percentage of pores of a given diameter in the VOI of samples 1-4 (Figure 16 a) and b)). Diameter was approximated by the diameter of the sphere of equivalent volume as the pore.

.

A similar plot tendency was observed for the cobblestone samples 20 and 21. Sample 21 also had a small percentage of bigger pores but sample 20 that came from the center of the cobblestone had a slightly higher percentage for pores greater than 0.36 mm in diameter. Both of these samples were compared to sample 22, a squared cobblestone. Samples from the same type of cobblestone follow a similar tendency, while sample 22 has a higher amount of small pores (Figure 21).

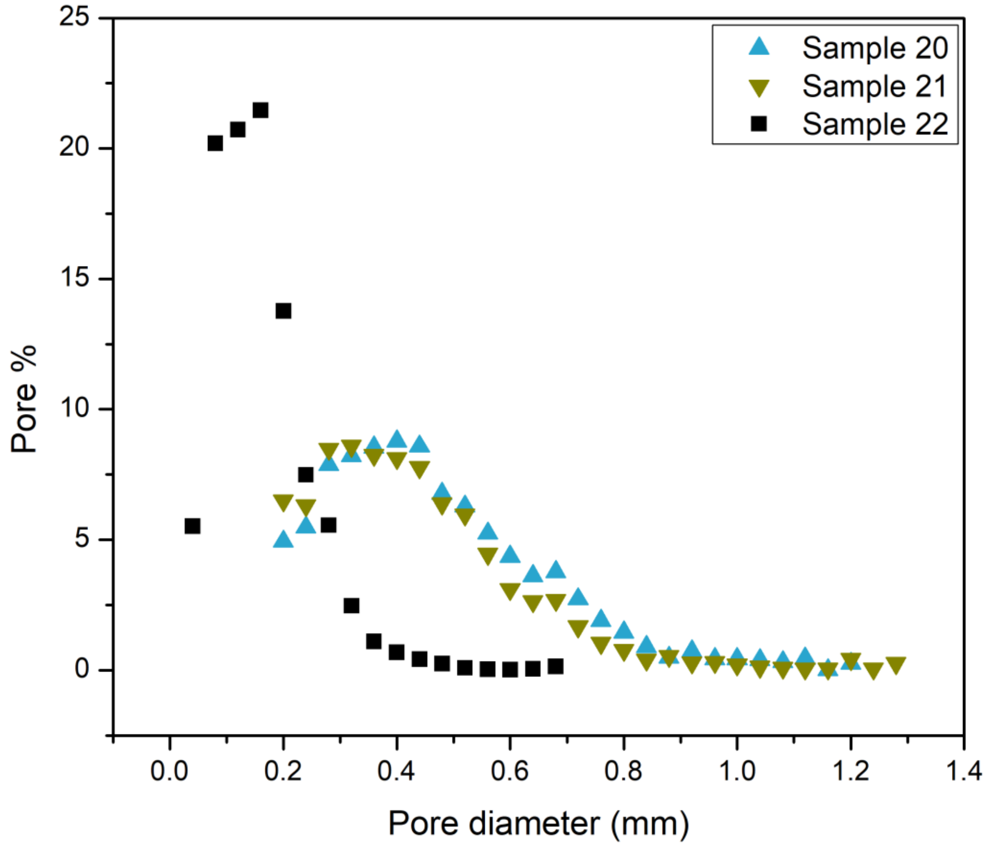

Figure 21: Percentage of pores of a given diameter in the VOI of samples 20-22. Diameter was approximated by the diameter of the sphere of equivalent volume as the pore.

Unlike the lava rocks and bricks, a preliminary view of sample 1 shows porosity without the need to amplify (Figure 22 a)). However, Figure 22 b) distinctively shows two small pores of around 160 µm in diameter near the edge of a larger particle. These pores are visibly deeper than in the case of previous samples. A longitudinal view of the pores along the sample seems to display an almost diagonal formation of pores from the surface (left side) to the deepest side of the core (right side) (Figure 22 d)). From the previous analysis, this diagonal formation of pores seems to support the theory that the pores migrate from the center, which is most likely the place with highest pore density.

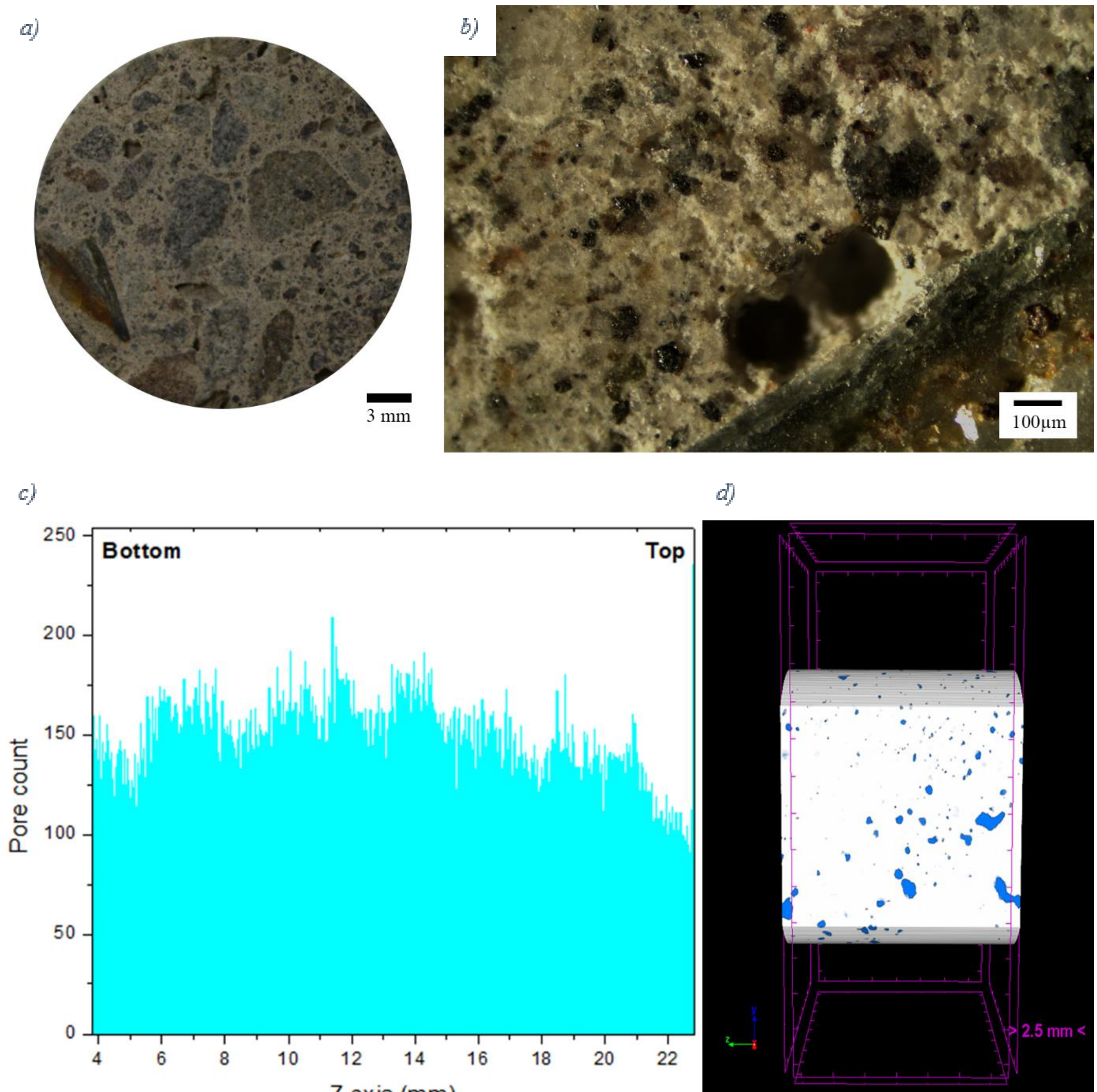

Figure 22:Different views of Sample 1. a) circular view of an interior side of the sample. b) view of the sample under a 5x increment lens. c) graph of the amount of pores along the Z axis. d) reconstructed sample in CTvox. Pores are highlighted in blue.

In the case of sample 21, a darker area with a slightly circular shape covered part of the center of the sample (Figure 23 a)). A closer look on that darker area shows an irregular pattern of macro pores which is not seen in the rest of the sample (Figure 23 b)). This gives the impression that this darkened area is indeed susceptible to a higher degree of damage.

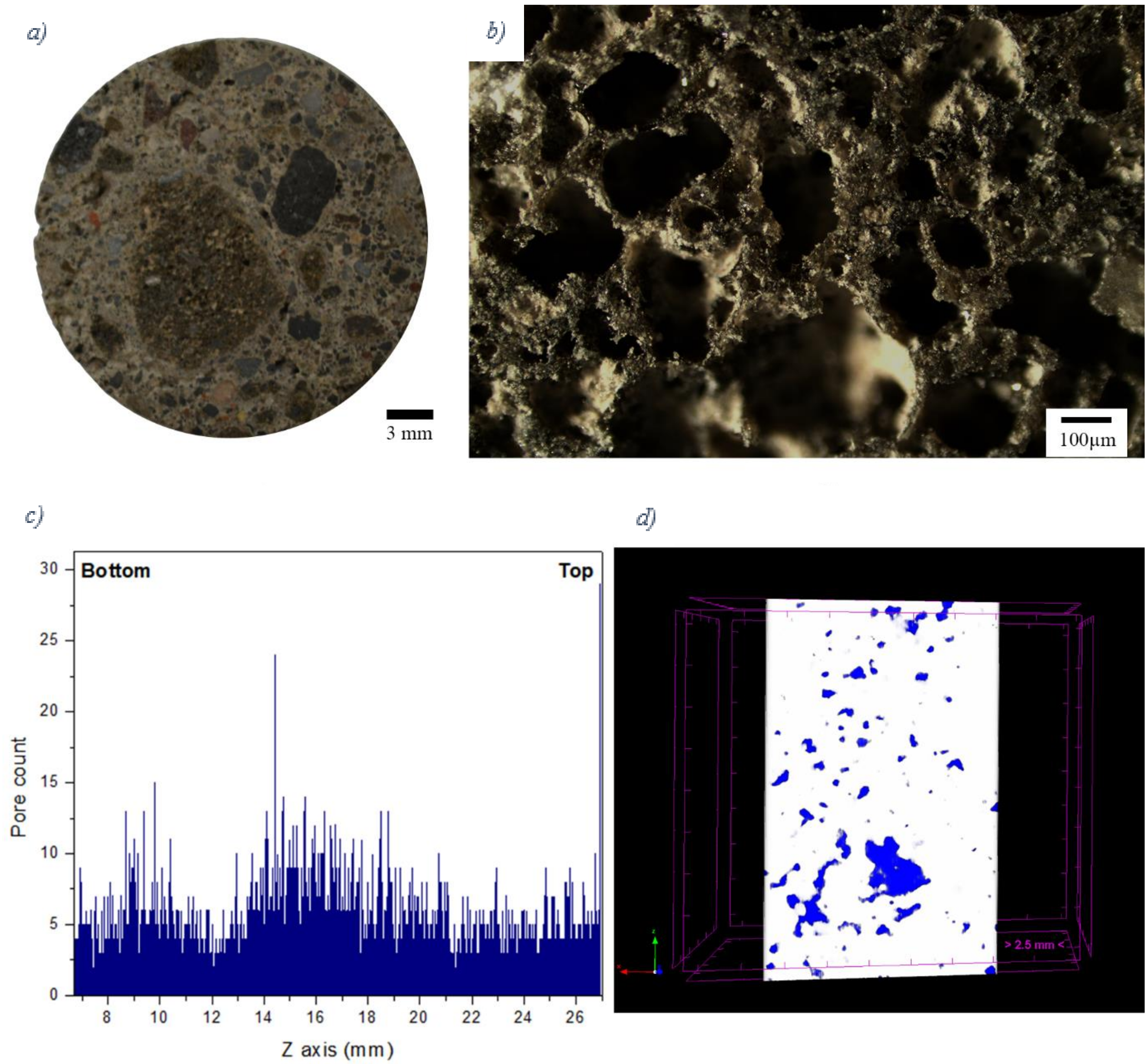

Figure 23: Different views of Sample 21. a) circular view of an interior side of the sample. b) view of the sample under a 5x increment lens over the darker area of the sample. c) graph of the amount of pores along the Z axis. Top (surface) and bottom of the sample are indicated in bold letters. d) reconstructed sample in CTvox. Pores are highlighted in blue.

By comparing the amount of pores of samples 1, 21 and 22 ((Figure 22 c), Figure 23 c) and Figure 24 c)) a similar trend remains in which a significantly larger number of pores rest on the surface of the sample. This analysis took into consideration that the depth of the pores on the surface was bigger than the width as to be considered a pore instead of just texture of the material.

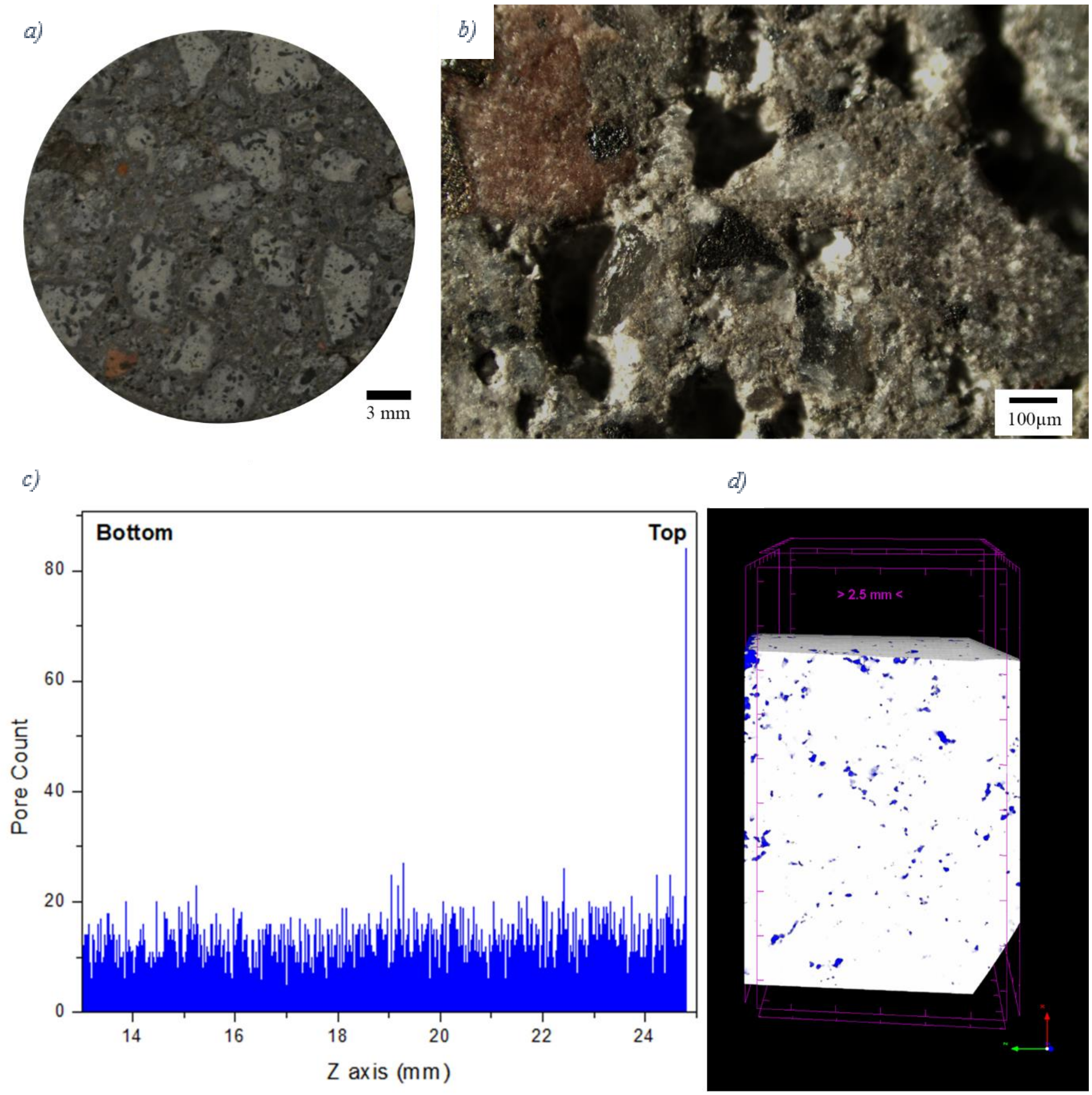

Figure 24: Different views of Sample 22. a) circular view of an interior side of the sample. b) view of the sample under a 5x increment lens. c) graph of the amount of pores along the Z axis. Top (surface) and bottom of the sample are indicated in bold letters. d) reconstructed sample in CTvox. pores are highlighted in blue.

4.5 CONCRETE

In the category of concrete, sample 30 had the lowest porosity in contrast with sample 17 that displayed the highest porosity (Figure 25). As explained in the sample acquisition, sample 17 came from a concrete wall covering a ravine. This location exposes the wall to a higher amount of water than for the other cases.

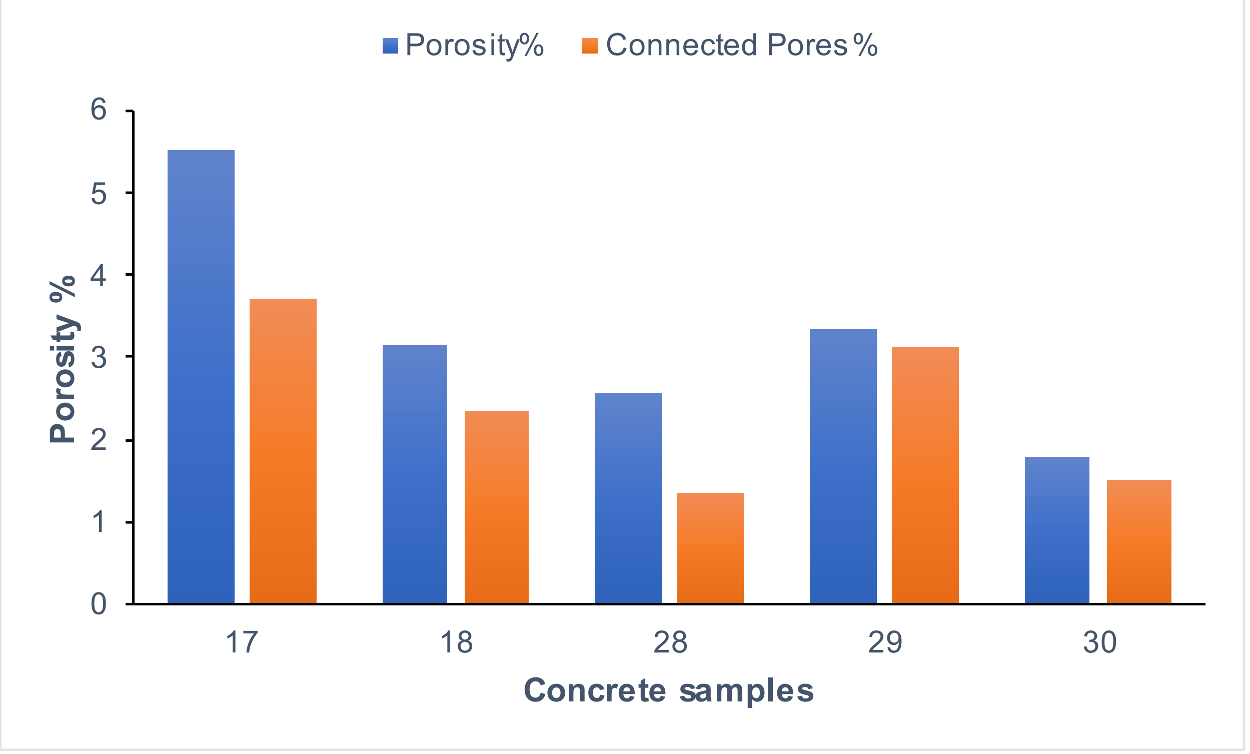

Figure 25: Percentage of porosity inside the VOI of the 5 concrete samples taken (see Figure 26). Total porosity is shown in blue, while only the connected pores are shown in orange.

As the primary agent of transportation for soluble salts, water causes the formation of pores. Furthermore, samples 28, 29 and 30 all came from similar sites yet sample 29 shows the highest porosity among them.

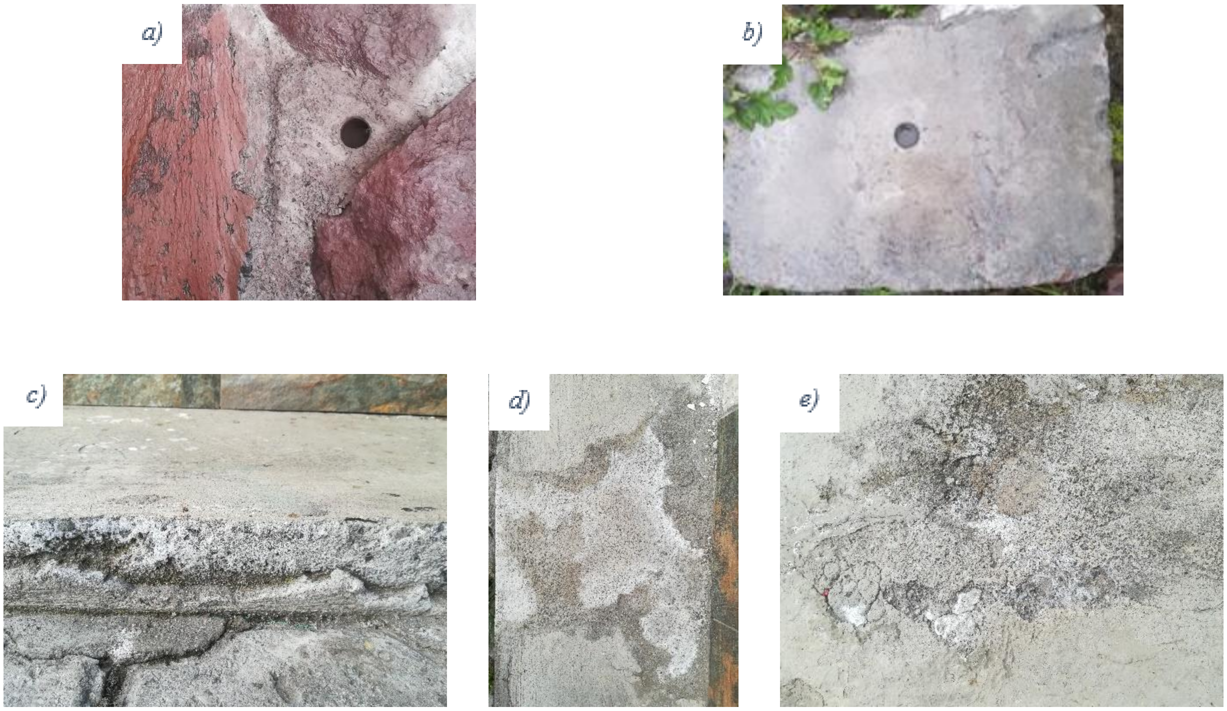

Figure 26: Extraction sites of 5 concrete samples. Sample 17 was taken from concrete used to cover a ravine wall, while samples 18, 28, 29 and 30 were taken from concrete blocks a) Sample 17. b) Sample 18. c) Sample 28 d) Sample 29 e) Sample 30.

From the extraction sites, samples 28 and 30 appear to be in similar deterioration conditions, with a rugged surface and irregular pattern of dark and white areas (Figure 26). And while these characteristics are shared with sample 29, they seem more pronounced for sample 29. This observation is merely based on the outer appearance of the source of each sample but it does coincide with the porosity calculated by micro-CT (Figure 25).

Conversely, samples 17 and 18 show a higher volume of pores compared to samples 28, 29 and 30. By analyzing the distribution of these pores, most of the pore volume for samples 17 and 18 are seen towards the surface of the samples (Figure 27). This seems to be due to higher exposure to moist environments (Figure 26 a) and b)). For samples 28, 29 and 30, though there are signs of haloclasty on the surface, this effect does not seem damaging enough on its own, given the fact that there is a considerable amount of larger pores much past the surface.

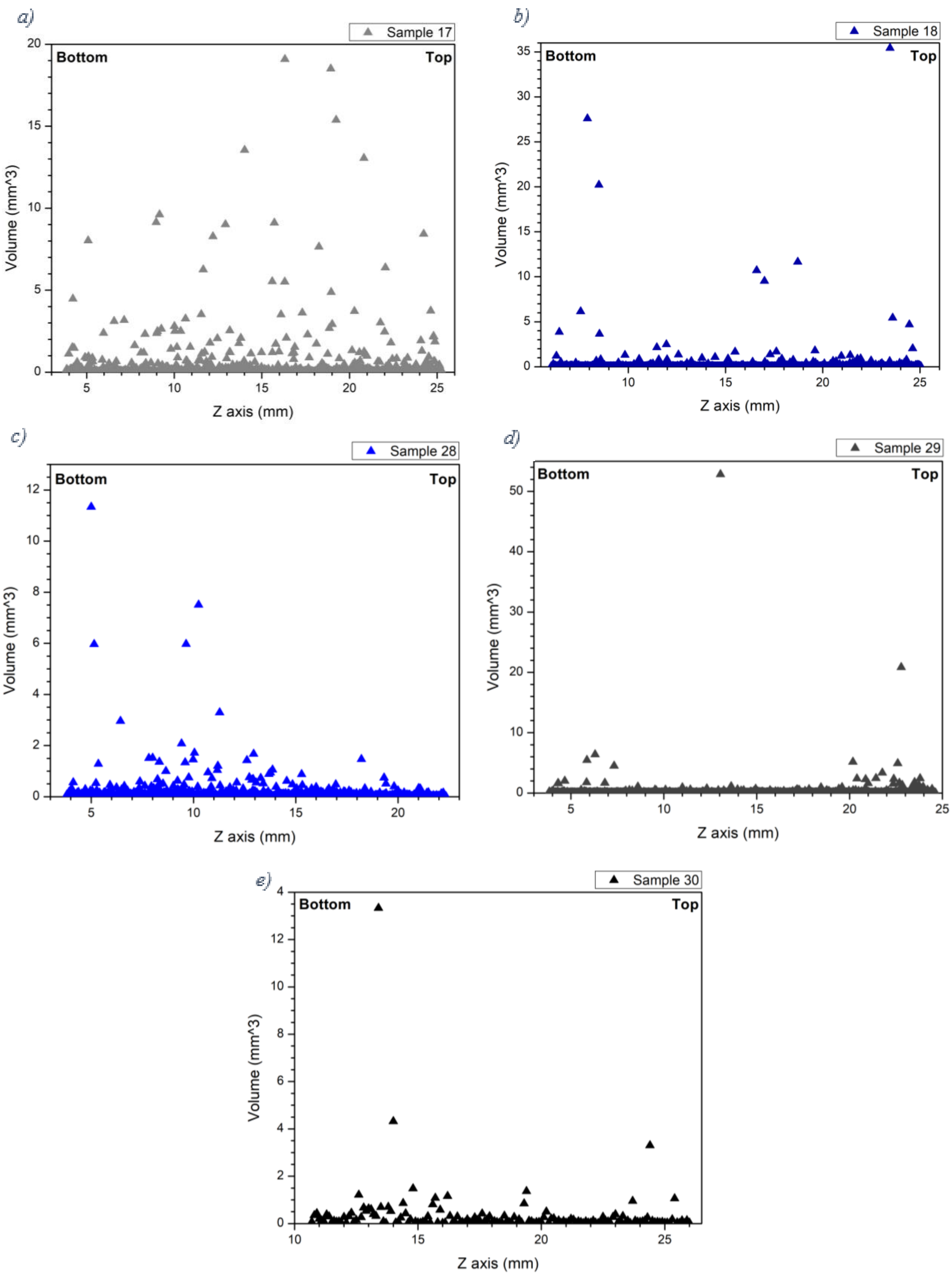

Figure 27: Pore volume longitudinal profile of concrete samples. Bottom and top of samples are indicated in bold letters. a)-e) Sum of pore volume along the Z axis for samples 17, 18, 28, 29 and 30.

4.6 SHAPE AND SIZE OF PORES

An individual analysis of pores revealed a strong correlation between the volume of the pores and the sphericity. Smaller pores tend to be more spherical than larger pores; and the largest pore volume tends to be towards the surface (Figure 28) This proved true specially for lava samples where the number of small pores detected was higher.

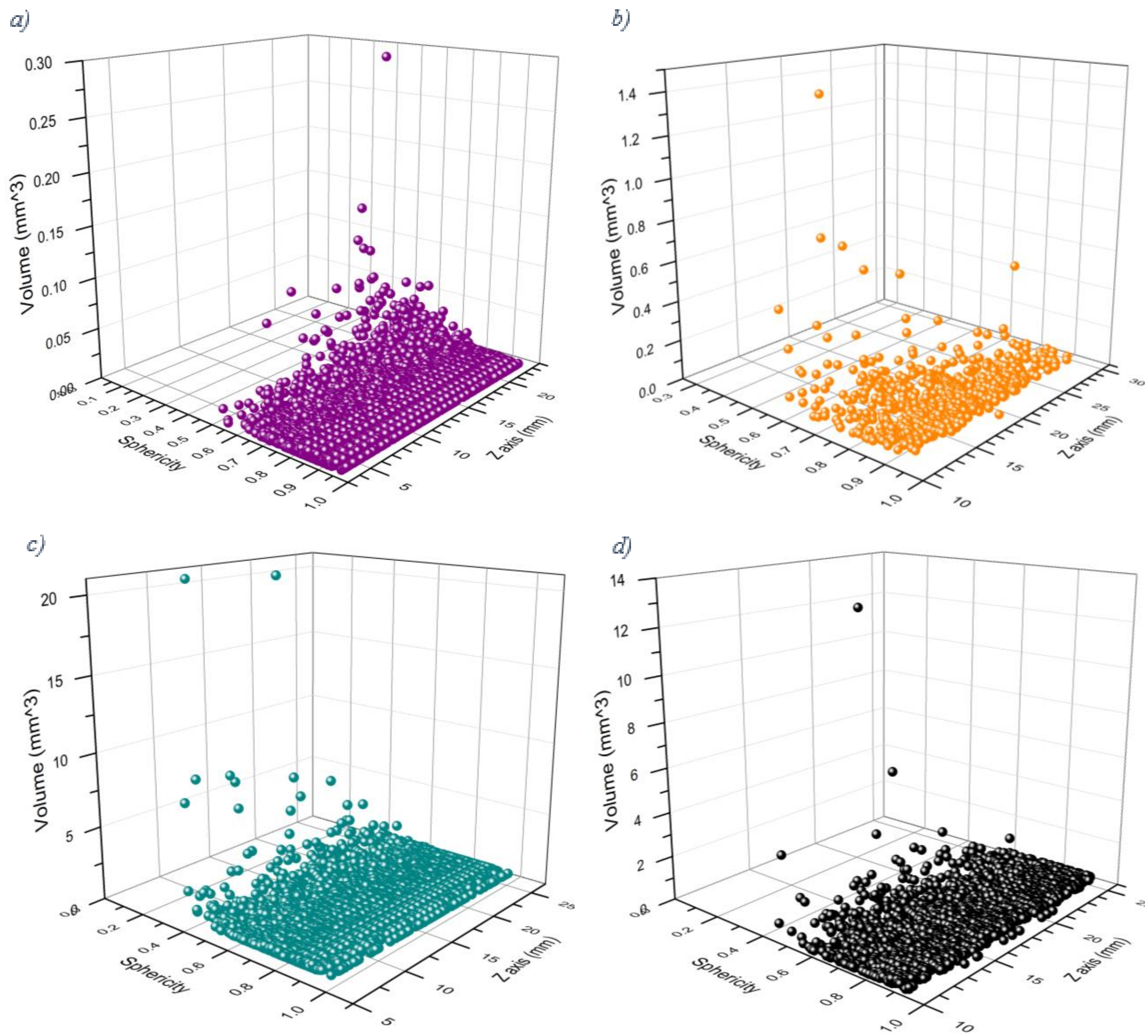

Figure 28: Sphericity and volume of pores along the Z axis. a) Lava rock sample 7 (Figure 8). b) Clay brick sample 19 (Figure 13) c) Cobblestone sample 21 (Figure 23). d) Concrete sample 30 (Figure 26e)).

4.7 DISCUSSION

Since the porosity of lava rocks is mostly secondary, these samples are a good point of comparison with the rest of the samples that are subjected to similar weathering conditions. Of all samples, bricks and lava rocks had the least amount of porosity calculated by the micro-CT method. For samples with initial low porosity, effects of haloclasty were barely observed. These results agree with another study in which salt crystallization was more prominent in rocks with higher porosity[68]. Though porosity is linked to certain physical properties of the materials, the lack of porosity does not immediately translate into a more durable material. Cobblestones had, in general, the highest porosity. Considering that the cobblestone samples were made from a mixture of concrete not much different to concrete blocks, it would seem odd that results are so different between the two categories. Yet this might be indicative to the effects that the environment has on each sample more than a difference in vulnerability. While cobblestones are designed by pressure on all external sides of the block, leaving space for pores towards the middle, rectangular blocks are usually made by compressing cement not only from all sides but also above.

The fact that pores were generally larger near the edges of bigger particles in the case of manmade materials is evidence of the formation of the materials with different grain sizes. The same was not observed in lava rock samples which form under great pressures.

Durability is an often sought out characteristic for construction materials, since it relates to how the material can withstand weathering and decay over time. Durability and strength are often linked with the lack of pores in the material and interlocking grains[18]. That said, resistance of a material like concrete is much more difficult to predict due to the complexity of its composition[69]. Particularly, some damage can be hidden beneath an undamaged mortar coating[39], therefore making the task of seeking out damaged infrastructure more difficult.

Bricks on the other hand, have less compressive strength than concrete, but depending on the environment, can be equally or more durable. It is known that bricks grow by the absorption of moisture. This growth is highly dependent on the firing process over the clay composition[19]. Damage to clay walls is a sign of lack of cohesion between the particles of the matrix of the brick.

This could indicate that brick samples taken were not high-quality bricks. Furthermore, the shape of the bricks did not seem uniform which does not contribute to an overall durable wall.

In some cases, the combination of mortar does not aid to the cohesion of the bricks. (Figure 11 b).

In order to study the effects of weathering, it’s useful to compare the initial rock, to certain intermediate stages and finally to the weathered product[42]. As found by Davison, haloclasty effects can be boosted by significant variation in temperature cycles, though not much debris was generated from samples subjected to a temperate climate, these samples were found to have a deeper penetration of salts. Additionally, haloclasty acted in different stages according to the degree of damage generated by the temperature cycles the samples were subjected to. This caused the generation of different sizes of debris according to each stage[70]. Though the samples chosen for this project showed signs of salts on the surface, the climate conditions of Ibarra resemble more temperate temperatures with slightly high levels of humidity[71], and the debris generated from the samples in no case seemed relevant, which implies that the effects produced by haloclasty were limited to an initial stage.

Finally, the determination of composition and crystalline phases with XRD was not made in order to allow further research on the samples without destroying them completely.

5 CONCLUSIONS

Micro-CT is a widely used method to analyze inner structures of samples with the advantage of being non-destructive. From the 30 samples analyzed, quantity, morphometry and distribution of porosity was closely studied. Clay brick samples and some lava rocks demonstrated microporosity, in particular, at the surface of each sample which was previously exposed to environmental conditions. Cobblestone samples all exhibited a higher amount of pores at the surface compared to the rest of the sample. Porosity was most accurately calculated for cobblestone and concrete samples while resolution proved to be problematic for brick samples.

6 RECOMMENDATIONS

This thesis centered on the analysis of samples limited to the city of Ibarra. The study contemplated the samples after noticeable deterioration yet further conclusions can be made by a comparison between the materials as they first settle against the deterioration that occurs time after, in order to observe the progress of deterioration over set intervals of time. Also, it would be beneficial to pick more samples that present the same effects to average the damage in each one.

For further investigations on the recollected samples in this thesis, petrographic analysis might provide further insight on the geological frame surrounding each sample. A combination of methods for porosity determination could serve to validate the results obtained by micro-CT. And finally, an XRD characterization might give more information on the results obtained in this thesis.

7 REFERENCES

(1) Segovia, M. D.; Yoris, A. I.; Guilarducci, A.; Defagot, C. A.; Ulibarrie, N. O. Carbonatación de Estructuras de Hormigón Armado En La Región Centro-Este Argentina: Influencia de La Contaminación Ambiental Urbana. *Revista Tecnología y Ciencia*. Santa Fe November 2009, p 14.

(2) Herrera Valdivieso, J. Estudio de Las Patologías En Elementos Constructivos de Albañilería Estructural, Aplicado En Un Proyecto Específico y Recomendaciones Para Controlar, Regular y Evitar Los Procesos Físicos En La Edificaciones Que Se Desarrollan En La Ciudad de Guayaquil, Universidad de Guayaquil, 2016.

(3) Cevallos, O. A.; Jaramillo, D.; Ávila, C.; Aldaz, X. Production and Quality Levels of Construction Materials in Andean Regions: A Case Study of Chimborazo, Ecuador. *J. Constr. Dev. Ctries.* **2017**, *22* (1), 115–136. https://doi.org/10.21315/jcdc2017.22.1.7.

(4) Ortiz, P. W. L. Influencia De La Humedad En El Deterioro De Las Viviendas Del Barrio Obrero De La Ciudad De Puyo, Cantón Pastaza, Provincia De Pastaza., Universidad Técnica de Ambato, 2011, Vol. 593.

(5) Chatelain, J. L.; Tucker, B.; Guillier, B.; Kaneko, F.; Yepes, H.; Fernandez, J.; Valverde, J.; Hoefer, G.; Souris, M.; Dupérier, E.; Yamada, T.; Bustamante, G.; Villacis, C. Earthquake Risk Management Pilot Project in Quito, Ecuador. *GeoJournal* **1999**, *49* (2), 185–196. https://doi.org/10.1023/A:1007079403225.

(6) Estupiñán Ricardo, J.; Domínguez Menéndez, J. J.; Barcos Arias, I. F.; Macías Bermúdez, J. M.; Moreno Lemus, N. Neutrosophic K-Means for the Analysis of Earthquake Data in Ecuador. *Neutrosophic Sets Syst.* **2021**, *44* (1), 29.

(7) Zulfikar, A. Why are earthquakes common in the Pacific Ring of Fire? https://www.dw.com/en/why-are-earthquakes-common-in-the-pacific-ring-of-fire/a-36676363 (accessed Jun 23, 2021).

(8) Mardon, A. A.; Haq, N.; Tang, M. *The Ring of Fire*; Golden Meteorite Press, 2021.

(9) Rodriguez, F.; Toulkeridis, T.; Sandoval, W.; Padilla, O.; Mato, F. Economic Risk Assessment of Cotopaxi Volcano, Ecuador, in Case of a Future Lahar Emplacement. *Nat. Hazards* **2017**, *85* (1), 605–618. https://doi.org/10.1007/s11069-016-2589-1.

(10) Blong, R. J. Volcanic Hazards Risk Assessment. *Monit. Mitig. Volcano Hazards* **1996**, 675–698. https://doi.org/10.1007/978-3-642-80087-0_20.

(11) 1,5 Millones de Ecuatorianos Viven Hacinados y En Casas 'Autoconstruidas.' *La Hora*. June 10, 2022.

(12) Remodelación y Reparación Empujan Al Sector de La Construcción. *El Comercio*. July 2021.

(13) APIVE. Materiales más demandados por el sector constructor ecuatoriano https://apive.org/materiales-mas-

demandados-por-el-sector-constructor-ecuatoriano/.

(14) *Construction Materials: Their Nature and Behaviour*, Third.; Illston, J. M., Domone, P. L. J., Eds.; Spon Press, 2001.

(15) Labahn, O.; Kohlhaas, B. Cement Engineer's Handbook. Bauverlag 1954, p 800.

(16) Bye, G. C. *Portland Cement Composition, Production and Properties*, Second.; Thomas Telford: London, 1999.

(17) Meade, R. K. *Portland Cement. Its Composition, Raw Materials, Manufacture, Testing and Analysis*, Third Edit.; The Chemical Publishing Company: London, 1926.

(18) McNally, G. *Soil and Rock Construction Materials*; 2017. https://doi.org/10.4324/9780203476574.

(19) *Clay Materials Used in Construction*; Reeves, G. M., Sims, I., Cripps, J. C., Eds.; The Geological Society of London, 2006.

(20) Ramachandran, V. S.; Paroli, R. M.; Beaudoin, J. J.; Delgado, A. H. *Handbook of Thermal Analysis of Construction Materials*; 2002; Vol. 406.

(21) Davidson, L.; Springman, S. Soil description and classification https://environment.uwe.ac.uk/geocal/SoilMech/classification/default.htm%0A%0A (accessed Nov 25, 2022).

(22) Antoniadis, K. D.; Assael, M. J.; Tsiglifisi, C. A.; Mylona, S. K. Improving the Design of Greek Hollow Clay Bricks. *Int. J. Thermophys.* **2012**, *33* (12), 2274–2290. https://doi.org/10.1007/s10765-012-1294-x.

(23) Brownell, W. E. *Structural Clay Products*, First Edit.; Springer Verlag, 1976; Vol. 2. https://doi.org/10.1155/tsm.2.257.

(24) What are Igneous rocks? https://www.usgs.gov/faqs/what-are-igneous-rocks#:~:text=Igneous rocks (from the Latin,then rises toward the surface. (accessed Nov 26, 2022).

(25) Earle, S. *Physical Geology*, Second.; BCcampus, 2019; Vol. 1986.

(26) What are metamorphic rocks? https://www.usgs.gov/faqs/what-are-metamorphic-rocks (accessed Nov 26, 2022).

(27) Wang, H.; Latham, J. P.; Poole, A. B. Predictions of Block Size Distribution for Quarrying. *Q. J. Eng. Geol.* **1991**, *24* (1), 91–99. https://doi.org/10.1144/GSL.QJEG.1991.024.01.10.

(28) Bosmediano, J.; Carbo, J. *Sector Cemento En El Ecuador*; Quito, 2015.

(29) Salvatierra, A.; Pérez, A.; Rodríguez, A. Estructura de Mercado Del Cemento En Ecuador de 2010 a 2020. *Rev. Coyunt. y Perspect.* **2022**, *7* (1), 15–20.

(30) Garófalo Mero, A. C. Evaluación Físico-Química de Los Cementos a Partir de La Correlación de Sus Propiedades Asociadas Con La Producción de Hormigón, Escuela Superior Politécnica del Litoral, 2015.

(31) Holcim. Locations https://www.holcim.com.ec/locations.

(32) UNACEM Ecuador https://www.linkedin.com/company/unacem-ecuador/.

(33) Buisiness Review America Latina. UCEM (Union Cementera Nacional). *Issuu*. April 2018.

(34) Cox Vásconez, A. E. Reglamento Técnico Ecuatoriano RTE INEN 007 (1R). Cementos, Cal y Yeso. Ministerio de Industrias y Productividad: Ecuador 2010, pp 5–7.

(35) *Cemento Portland. Requisitos*; Quito, Ecuador, 2010; Vol. 152.

(36) *Cemento Hidráulico. Definición de Términos.*; Quito, 2010; Vol. 151.

(37) NTE INEN 490. Cementos Hidráulicos Compuestos. Requisitos. *Inst. Ecuatoriano Norm.* **2011**, 17.

(38) Chian, S. C.; Wilkinson, S. M.; Whittle, J. K.; Mulyani, R.; Alarcon, J. E.; Pomonis, A.; Saito, K.; Fraser, S.; Goda, K.; Macabuag, J.; Offord, M.; Hunt-Raby, A. C.; Sammonds, P.; Franco, G.; Stone, H.; Ahmed, B.; Hughes, F. E.; Jirouskova, N. K.; Kaminski, S.; Lopez, J. Lessons Learnt from the 2009 Padang Indonesia, 2011 Tōhoku Japan and 2016 Muisne Ecuador Earthquakes. *Front. Built Environ.* **2019**, *5* (June), 1–20. https://doi.org/10.3389/fbuil.2019.00073.

(39) Yépez, F.; Yépez, O. Role of Construction Materials in the Collapse of R/C Buildings after Mw 7.8 Pedernales – Ecuador Earthquake, April 2016. *Case Stud. Struct. Eng.* **2017**, *7* (April), 24–31. https://doi.org/10.1016/j.csse.2016.12.001.

(40) Wilson, T. M.; Jenkins, S.; Stewart, C. *Impacts from Volcanic Ash Fall*; Elsevier Inc., 2015. https://doi.org/10.1016/B978-0-12-396453-3.00003-4.

(41) Blong, R. J.; Grasso, P.; Jenkins, S. F.; Magill, C. R.; Wilson, T. M.; McMullan, K.; Kandlbauer, J. Estimating Building Vulnerability to Volcanic Ash Fall for Insurance and Other Purposes. *J. Appl. Volcanol.* **2017**, *6* (1). https://doi.org/10.1186/s13617-017-0054-9.

(42) Parry Reiche. Graphic Representation of Chemical Weathering. *J. Sediment. Petrol.* **1943**, *Vol. 13* (2), 58–68. https://doi.org/10.1306/d4269198-2b26-11d7-8648000102c1865d.

(43) Camuffo, D. Physical Weathering of Stones. *Sci. Total Environ.* **1995**, *167* (1–3), 1–14. https://doi.org/10.1016/0048-9697(95)04565-I.

(44) Taylor, L. L.; Leake, J. R.; Quirk, J.; Hardy, K.; Banwart, S. A.; Beerling, D. J. Biological Weathering and the Long-term Carbon Cycle Integrating Mycorrhizal Evolution and Function into the Current Paradigm. *Geobiology* **2009**, *7*, 171–191.

(45) Doornkamp, J. C.; Ibrahim, H. A. M. Salt Weathering. *Prog. Phys. Geogr.* **1990**, *14* (3), 335–348. https://doi.org/10.1177/030913339001400303.

(46) *Geomorphology of Desert Environments*, First.; Abrahams, A. D., Parsons, A. J., Eds.; Springer, 1994; Vol. 4.

(47) *Guide To Durable Concrete.*; 1977; Vol. 74. https://doi.org/10.14359/11047.

(48) Jin, P. jun; Zhang, Y.; Wang, S.; Yang, X. gang; Zhang, M. Characterization of the Superficial Weathering of Bricks on the City Wall of Xi'an, China. *Constr. Build. Mater.* **2017**, *149*, 139–148. https://doi.org/10.1016/j.conbuildmat.2017.05.045.

(49) Charola, A. E. Salts in the Deterioration of Porous Materials: An Overview. *J. Am. Inst. Conserv.* **2000**, *39* (3), 327–343. https://doi.org/10.1179/019713600806113176.

(50) Klenz Larsen, P. The Salt Decay of Medieval Bricks at a Vault in Brarup Church, Denmark. *Environ. Geol.* **2007**, *52* (2), 375–383. https://doi.org/10.1007/s00254-006-0586-5.

(51) Price, C. A. *Stone Conservation: An Overview of Current Research*, First Edit.; The Getty Conservation Institute, 1996.

(52) Chung, S. Y.; Lehmann, C.; Elrahman, M. A.; Stephan, D. Pore Characteristics and Their Effects on the Material Properties of Foamed Concrete Evaluated Using Micro-CT Images and Numerical Approaches. *Appl. Sci.* **2017**, *7* (6). https://doi.org/10.3390/app7060550.

(53) Nambiar, E. K. K.; Ramamurthy, K. Sorption Characteristics of Foam Concrete. *Cem. Concr. Res.* **2007**, *37* (9), 1341–1347. https://doi.org/10.1016/j.cemconres.2007.05.010.

(54) Rouquerol, J.; Avnir, D.; Fairbrigne, C. W.; Everett, D. H.; Haynes, J. H.; Pericone, N.; Ramsay, J. D. F.; Sing, K. S. W.; Unger, K. K. *Recommendations for the Characterization of Porous Solids*; 1994; Vol. 66. https://doi.org/10.1016/S0022-460X(03)00515-7.

(55) Porosity. In *The IUPAC Compendium of Chemical Terminology*; IUPAC, 2014; Vol. 71, p 4762. https://doi.org/10.1351/goldbook.p04762.

(56) Koenig, A. Analysis of Air Voids in Cementitious Materials Using Micro X-Ray Computed Tomography (MXCT). *Constr. Build. Mater.* **2020**, *244*, 118313. https://doi.org/10.1016/j.conbuildmat.2020.118313.

(57) Doehne, E. Salt Weathering: A Selective Review. *Geol. Soc. Spec. Publ.* **2002**, *205*, 51–64. https://doi.org/10.1144/GSL.SP.2002.205.01.05.

(58) Wikipedia Contributors. Ibarra, Ecuador https://en.wikipedia.org/wiki/Ibarra,_Ecuador#cite_note-1 (accessed Feb 20, 2023).

(59) *Fascículo Provincial Imbabura*; 2010.

(60) Ibarra https://vivatravelguides.com/ecuador/ibarra/ (accessed Feb 20, 2023).

(61) Imbabura Datos Generales https://www.imbabura.gob.ec/index.php/imbabura/datos-generales#:~:text=Los tipos de clima presentes,sector de Íntag y Lita. (accessed Nov 10, 2022).

(62) Clima Ibarra (Ecuador) https://es.climate-data.org/america-del-sur/ecuador/provincia-de-imbabura/ibarra-2964/ (accessed Nov 10, 2022).

(63) *Cargas Sísmicas. Diseño Sismo Resistente*.

(64) Stein, K.; Sander, M. HISTOLOGICAL CORE DRILLING: A LESS DESTRUCTIVE METHOD FOR STUDYING BONE. In *Methods in Preparation: Proceedings of the First Annual Fossil Preparation and Collections Symposium*; Brown, M. A., Kane, J. F., Parker, W. G., Eds.; 2009; Vol. 1, pp 69–80.

(65) Sijbers, J.; Postnov, A. Reduction of Ring Artefacts in High Resolution Micro-CT Reconstructions. *Phys. Med. Biol.* **2004**, *49* (14). https://doi.org/10.1088/0031-9155/49/14/N06.

(66) BRUKER Skyscan 2211 Micro-CT Scanner Specifications : Université de Fribourg 2014, p 2211.

(67) Brooks, R. A.; Di Chiro, G. Beam Hardening in X-Ray Reconstructive Tomography. *Phys. Med. Biol.* **1976**, *21* (3), 390–398. https://doi.org/10.1088/0031-9155/21/3/004.

(68) Jamshidi, A.; Nikudel, M. R.; Khamechiyan, M. Estimating the Durability of Building Stones against Salt Crystallization: Considering the Physical Properties and Strength Characteristics. *Geopersia* **2013**, *3* (2), 35–48.

(69) López Orozco, J. O. Porosidad Del Concreto, Universidad de San Carlos de Guatemala, 2004.

(70) Davison, A. P. An Investigation into the Relationship between Salt Weathering Debris Production and Temperature. *Earth Surf. Process. Landforms* **1986**, *11* (3), 335–341. https://doi.org/10.1002/esp.3290110311.

(71) Scacco Carrasco, A. *Actualización Del Plan De Desarrollo Y Ordenamiento Territorial Del Cantón Ibarra*; Ibarra, 2020.

8 ANNEXES

Annex 1: Specifications used in sample imaging

Samples	Voltage [kV]	Current [µA]	Exposure [ms]	Rotation [deg]
1	90	140	70	0.300
2	90	140	70	0.300
3	90	140	70	0.300
4	90	140	70	0.300
5	90	140	70	0.300
6	90	140	70	0.200
7	90	140	70	0..300
8	90	100	100	0.200
9	100	140	100	0.200
10	80	140	100	0.200
11	50	200	250	0.500
12	100	100	100	0.200
13	100	100	100	0.200
14	100	100	100	0.200
15	100	100	100	0.200
16	100	100	100	0.200
17	80	100	200	0.500
18	90	170	200	0.500
19	100	170	140	0.500
20	90	170	200	0.500
21	90	150	200	0.500
22	90	170	200	0.500
23	70	150	200	0.500
24	80	150	200	0.500
25	80	150	200	0.500
26	80	150	200	0.500
27	80	150	200	0.500
28	80	200	200	0.500
29	80	200	200	0.500
30	80	200	200	0.500

Annex 2: Reconstruction parameters in NRecon

Samples	Postalignment	Smoothing	Ring Artifacts	Beam hardening
1	0.00	5	18	30
2	1.50	10	28	40
3	-0.50	3	23	75
4	0.00	2	40	41
5	-0.50	0	31	25
6	0.00	4	14	25
7	-1.50	6	20	25
8	-0.50	5	19	25
9	3.00	7	15	25
10	-5.00	3	15	28
11	-0.50	3	15	25
12	-0.50	7	15	35
13	-2.50	2	15	25
14	0.00	5	7	25
15	1.50	6	5	25
16	1.00	1	5	15
17	-0.50	5	5	25
18	-0.50	5	5	25
19	-0.50	4	5	25
20	-1.50	5	5	25
21	0.00	5	5	25
22	-1.50	5	7	25
23	-1.50	4	5	25
24	0.00	5	7	25
25	-1.50	5	7	25
26	-0.50	5	7	25
27	0.00	5	7	25
28	-1.50	3	5	25
29	0.00	5	5	20
30	-1.50	4	5	25